NASA TECHNICAL MEMORANDUM

NASA TM X-62,057

NASA TM X-62,057

AERODYNAMIC HEATING OF A SPACE SHUTTLE DELTA–WING ORBITER

William K. Lockman and Charles E. DeRose

Ames Research Center
Moffett Field, Calif. 94035

August 1971

AERODYNAMIC HEATING OF A SPACE SHUTTLE DELTA-WING ORBITER

By

William K. Lockman and Charles E. DeRose
Ames Research Center

ABSTRACT

An experimental investigation was performed to obtain detailed aerodynamic heating distributions on a model of a space-shuttle delta-wing orbiter with twin wing-tip vertical tails. Test data were obtained for an angle-of-attack range of -5° to 53°, selected sideslip and control-surface deflection angles, a free-stream Mach number of 7.4, and free-stream Reynolds numbers, based on model body length, from 1×10^6 to 7×10^6. Results showing the effects of Reynolds number, vehicle attitude, and control-surface deflections on the vehicle heating are presented and analyzed.

AERODYNAMIC HEATING OF A SPACE SHUTTLE DELTA-WING ORBITER

By

William K. Lockman and Charles E. DeRose
Ames Research Center

SUMMARY

An experimental investigation was performed to obtain detailed aerodynamic heating distributions on a space shuttle delta-wing orbiter model. The test model, instrumented with thermocouples, was a 0.006-scale representation of the North American Rockwell Corporation 134B delta-wing orbiter with twin wing-tip vertical tails. The test program was conducted in the Ames 3.5-foot hypersonic wind tunnel for an angle-of-attack range of -5° to 53°, selected sideslip and control-surface deflection angles, a free-stream Mach number of 7.4, and free-stream Reynolds numbers, based on model body length, from 1×10^6 to 7×10^6.

Complete tabulated results for the test program are included and representative plotted results are presented and discussed to show the effects of Reynolds number, vehicle attitude (angle of attack and sideslip angle), and control-surface deflections (elevon and rudder) on the vehicle heating distributions. For angles of attack from 15° to 53°, the laminar heating for the bottom centerline of the body forward of the wing, except for the nose stagnation region, were predicted well by modified swept-cylinder theory. Usually, the effect of increasing angle of attack was to increase the heating on the windward surfaces and decrease the heating on the leeward surfaces where flow separation occurred. On the windward surfaces of the body and wing, increasing Reynolds number caused increases in heating, thus indicating the possibility of boundary-layer transition and/or the effects of the complex flow in the wing-body shock layer. Increases in heating with increasing Reynolds number were also observed in regions where reattaching flow occurred, such as on the canopy. Increasing sideslip angle (windward) and deflecting control surfaces into the windward flow caused marked increases in heating on the body side and the control surfaces, respectively.

INTRODUCTION

Fully reusable two-stage space shuttle systems, to be used for transporting payloads from earth to low-earth orbit and return, are currently being investigated (see reference 1). The first stage of such a shuttle system is a booster that will provide initial acceleration for the system, and the second stage is an orbiter, containing the payload, that will continue into orbit. Both of these stages must be capable of returning to the launch site - or other predetermined location - and making conventional airplane-type landings.

Successful development of such a shuttle system requires the understanding of problems in many technological areas. For example, configuration definition and reusability for both the booster and the orbiter are dependent on a complete knowledge of the aerodynamic heating of these vehicles for their broad range of flight conditions. In particular, this requires a large body of heating data to provide a data base for the development and/or evaluation of various techniques for predicting the aerodynamic heating to shuttle vehicles.

The present experimental investigation was thus performed to obtain detailed aerodynamic-heating distributions on a delta-wing orbiter model for a range of test conditions. The test model, instrumented with thermocouples, was provided by North American Rockwell Corporation (NAR) and was a 0.006-scale representation of the NAR 134B delta-wing orbiter with twin wing-tip vertical tails. The test program was conducted in the Ames 3.5-foot hypersonic wind tunnel for an angle-of-attack range of -5° to 53° at a free-stream Mach number of 7.4 and free-stream Reynolds numbers, based on model body length, from 1×10^6 to 7×10^6. Results showing the effects of Reynolds number, vehicle attitude (angle of attack and sideslip angle), and control-surface deflections (elevon and rudder) on the vehicle heating distributions are presented and some comparisons with theory are shown. Some of these test results and analyses have already been presented in references 2 and 3. The photographs in reference 4 showing the surface oil-flow patterns on the NAR 129 delta-wing orbiter, which is similar to the NAR 134B configuration, were helpful in interpreting the test results.

The authors gratefully acknowledge the help of Harold Gorowitz and Patrick Carroll from North American Rockwell Corporation in the performance of the tunnel test program.

NOMENCLATURE

c	specific heat of model skin material
H	total enthalpy
L	model reference length (body axial length)
M_∞	free-stream Mach number
p	pressure
$\dot{q}$	heat-transfer rate
$\dot{q}_w$	heat-transfer rate at model wall

$\dot{q}_s$	stagnation-point heat-transfer rate for reference sphere
r	local chine radius of body
R_b	local half-width of body
R_s	reference sphere radius, 0.183 cm (0.006 ft) for test, equivalent to 0.305 m (1 ft) for full-scale vehicle
$Re_{\infty,L}$	free-stream Reynolds number based on model reference length, L
s	surface distance in cross-flow direction
T	temperature
t	time
u	cross-flow velocity at edge of boundary layer
x	body axial distance from nose
α	angle of attack
β	sideslip angle
δ_e	elevon deflection angle (positive with trailing edge down)
δ_r	rudder deflection angle (positive with trailing edge to left)
ϵ	surface emissivity
ϕ	body circumferential angle (positive measured clockwise from bottom centerline as viewed from rear of model)
ρ	density of model skin material
τ	thickness of model skin

Subscripts:

aw	adiabatic wall
cyl	cylinder stagnation line
ℓ	local value
L	based on body axial length
s	reference sphere
sl	symmetry or stagnation line
t	free-stream total condition
w	wall
∞	free-stream static condition

EXPERIMENTAL METHOD

Facility

The test program was conducted in air in the Ames 3.5-foot hypersonic wind tunnel. This facility, described in reference 5, is a blowdown-type tunnel that utilizes a pebble-bed heater to heat the air and axisymmetric contoured nozzles to provide flow Mach numbers of 5.2, 7.4, and 10.4. The nozzle walls are insulated from the hot airstream by injecting helium into the nozzle boundary layer through annular slots upstream of the throat. The tunnel is equipped with a model quick-insert mechanism for quickly moving models into and out of the airstream.

A high-speed analog-to-digital data acquisition system is used to record test data on magnetic tape. The present system is equipped to measure and record the outputs from 80 thermocouples and/or other types of transducers in addition to 20 channels of tunnel parameters.

Model

The test model, provided by North American Rockwell Corporation (NAR or NR), was a 0.006-scale representation of the NAR 134B delta-wing orbiter. A photograph of the model, and a three-view drawing of the model showing the principal dimensions and flow orientation are given in figures 1 and 2, respectively. Tabulated dimensional data, provided by NAR, for both the full-scale and model-scale delta-wing orbiters are given in Appendix A.

The basic model geometry consisted of a fuselage body (B_5), a blended delta wing (W_{15}) with deflectable elevons (E_5), and twin wing-tip vertical tails (V_{15}) with deflectable rudders (R_5). Replaceable brackets were used to vary the elevon deflection angles (-7.5°, 0°, 10° and 14°) and rudder deflection angles (0°, $\pm 13^\circ$, and $\pm 20^\circ$). Both the left (+) and right (-) rudder deflections were only outboard.

The model was constructed of 17-4 PH stainless steel and had the instrumented areas machined to a nominal skin thickness of 1 millimeter (0.040 in.). The actual skin thickness was measured at each instrumented location. Model instrumentation consisted of 92 iron-constantan thermocouples (30-gage wire) spot welded to the inner surface of the model at the locations listed in Table I and shown in Figure 3. The 80 thermocouples (T/C) listed in Table II were connected to the data acquisition system for this test program.

Test Conditions

The test program which is presented in Table III was conducted at a free-stream Mach number of 7.4 for a range of free-stream Reynolds numbers, based on model body length, between 1×10^6 and 7×10^6. The Reynolds number of 1×10^6 corresponds to the value for the full-scale vehicle near peak heating. The

maximum Reynolds number was limited to 4×10^6 at an angle of attack of 53° because of strength limitations of the model. Data were obtained for an angle-of-attack range of -5° to 53°, with emphasis on the entry values of 15°, 30°, and 53°. Tests were made at $\alpha = 15^\circ$, 30°, and 53° with sideslip angles of 0° and -5° (instrumented lift side of model windward) and with selected control-surface deflections (δ_e and δ_r) as shown in Table III. The runs at $\alpha = -5^\circ$ and 0 provide orbiter-alone data as baseline information for the orbiter mated to a booster as a launch configuration.

The specific test conditions, including the tunnel free-stream total temperature and pressure, are given for each run in Appendix B. The run data are given in the order of the run schedule given in Table III.

Test Procedures and Data Reduction

The model was mounted with a base sting at a preset attitude on the quick-insert mechanism. This mechanism injected the model into the airstream when steady-state test conditions were established and retracted the model at the completion of data acquisition. The model injection and retraction times were each set at about 1/2 second and the time on the tunnel centerline was set at about 1 second.

The model wall temperature data for each thermocouple location and the tunnel conditions were recorded on magnetic tape at 0.07-second intervals during the test duration of about 2 seconds. The resulting wall temperatures were differentiated with respect to time on a digital computer and the wall heat-transfer rate, $\dot{q}_w$, was then determined by the thin-skin technique with the following heat-balance equation:

$$\dot{q}_w = \rho c \tau \frac{dTw}{dt} \tag{1}$$

The data reduction program yields, for each thermocouple location, tabulated and plotted outputs of both wall temperature and heat-transfer rate versus time. Heat conduction errors in the model skin at any given location were minimized by using the data obtained at the earliest possible time after the model cleared the tunnel boundary layer into the free stream. This minimum time was influenced primarily by the combined effects of the model material response time (about 0.1 second) and the model transit time (dependent on model attitude) through the tunnel boundary layer. As would be expected, heat-conduction effects were generally limited to regions with small radii of curvature where large temperature gradients were present, such as the fuselage nose, wing leading edges, and tail leading edges.

To provide a convenient reference, the measured heating rates were normalized by the theoretical stagnation-point heating rate for a sphere (reference 6), $\dot{q}_s$, with a radius equivalent to 0.305-meter (1 foot) on the full-scale vehicle. The value of $\dot{q}_s$ for each run (Appendix B) was evaluated for the measured wind-tunnel test conditions. The wall temp-

erature used for the calculation of $\dot{q}_s$ was that for a fuselage nose thermocouple when the model reached the tunnel centerline. Therefore, the sphere wall temperature was generally higher than the model temperatures determined at the earlier times when the model heating rates were evaluated. However, the higher sphere temperature gave a smaller value of $\dot{q}_s$ and thus a larger, or more conservative, value for the heating-rate ratio, $\dot{q}_w/\dot{q}_s$. This effect was usually less than 10 percent and within the experimental accuracy. The estimated maximum error in the heating-rate ratio, $\dot{q}_w/\dot{q}_s$, is $\pm$ 10 percent for $\dot{q}_w/\dot{q}_s \geq 0.01$ and $\pm$ 0.002 for $\dot{q}_w/\dot{q}_s < 0.01$.

The calculations of both the reference sphere heating and the Reynolds number included the use of Keyes' equation for viscosity (see reference 7), and the corrections of reference 8 for calorically imperfect, thermally perfect gas.

MODIFIED SWEPT-CYLINDER THEORY

Laminar heat-transfer data obtained on the centerline of the body windward surface at angle of attack are later compared with predictions using infinite swept-cylinder theory (references 9 and 10) modified to account for the difference in cross-flow velocity gradient between the actual body and a cylinder.

A ratio of the heat-transfer rate for the symmetry or stagnation line of the windward surface at any local angle of attack α_ℓ to that for the reference sphere can be expressed by the following identity:

$$\frac{\dot{q}_{sl,\alpha_\ell}}{\dot{q}_s} = \left[\frac{\dot{q}_{cyl,\ \alpha_\ell = 90^\circ}}{\dot{q}_s}\right]\left[\frac{\dot{q}_{cyl,\ \alpha_\ell}}{\dot{q}_{cyl,\ \alpha_\ell=90^\circ}}\right]\left[\frac{\dot{q}_{sl,\ \alpha_\ell}}{\dot{q}_{cyl,\alpha_\ell}}\right] \tag{2}$$

Substituting expressions from reference 9 for the first and third bracketed terms and from reference 10 for the second term, results in

$$\frac{\dot{q}_{sl,\ \alpha_\ell}}{\dot{q}_s} = \left[\frac{(R_s/R_b)^{1/2}}{1.4}\right]\left[(\sin 1.1\alpha_\ell)\ \frac{H_{aw}-H_w}{H_t-H_w}\right]\left[\frac{(du/ds)_{sl}}{(du/ds)_{cyl}}\right]^{1/2}_{\alpha_\ell} \tag{3}$$

The adiabatic wall enthalpy for the stagnation line of a swept cylinder, H_{aw}, is given by the following equation for high free-stream velocities (reference 9):

$$\frac{H_{aw}}{H_t} = 1 - 0.15\cos^2\alpha_\ell \tag{4}$$

where the value of the recovery factor was taken as 0.85. The last bracketed term in equation (3), the ratio of the cross-flow velocity gradient for the actual body to that for a cylinder of the same dimension, can be calculated analytically by the method of integral relations discussed in reference 11. However, for this study, the following simple geometric correlation from reference 12 was used for the velocity-gradient term:

$$\frac{(du/ds)_{sl}}{(du/ds)_{cyl}} = \frac{0.745 + 1.57\ (r/R_b)}{2.315} \qquad (5)$$

where r and R_b are the chine radius and half-width, respectively, of the body.

RESULTS AND DISCUSSION

Complete results for the test program presented in Table III are tabulated in Appendix B. For each run, these results include both the wall temperature, T_w, and the heating-rate ratio, $\dot{q}_w/\dot{q}_s$, for each specified thermocouple location on the model, and the particular test conditions for the run.

Representative heating-rate distributions for the body, wing, and twin vertical tails will be presented and discussed for the entry angle-of attack range from 15° to 53°. Corresponding estimates of the radiation equilibrium surface temperatures for the full-scale vehicle at peak heating rate along a typical trajectory with the vehicle at $\alpha = 30^\circ$ will also be given for reference. For this typical trajectory, $\dot{q}_s = 681$ KW/m^2 (60 Btu/ft^2-sec) and $\varepsilon = 0.8$. As previously mentioned, the test Reynolds number of 1×10^6 corresponds to the value for the full-scale vehicle near peak heating.

Body

Body heating data for the bottom centerline, the top centerline, the side ($\phi \approx 100^\circ$), and various cross sections are presented in figures 4 to 6, 7, 8, and 9, respectively.

Bottom centerline.- Heating rates for the bottom centerline of the body at $\alpha = 15^\circ$, 30°, and 53° are plotted in figure 4 for Reynolds numbers between 1×10^6 and 7×10^6. As previously mentioned, the maximum Reynolds number for $\alpha = 53^\circ$ was limited to 4×10^6. The data for the low Reynolds numbers appear to be laminar for all three angles of attack. However, the data for the higher Reynolds numbers show an increase in heating with an increase in Reynolds number, indicating that transition to turbulent boundary-layer flow occurs. These effects at the higher Reynolds number could be influenced by the interaction of the wing-body shock layer with the body boundary layer (see, e.g., reference 13) and by the boattailing of the body surface starting at about $x/L = 0.8$. In addition, surface roughness effects on boundary-layer transition must be considered (see reference 3). Further discussion of transition results is given later in this section.

At each angle of attack shown in figure 4, the laminar heating rates decrease with distance from the stagnation region, remain relatively constant over the flat portion of the body, and then decrease at x/L greater than 0.8 where the body boattailing occurs. Predictions of the laminar heating rates ahead of the wing by modified swept-cylinder theory (i.e., equations (3), (4), and (5)) are shown for each angle of attack. The predicted values agree well with the data except for the noze stagnation region ahead of x/L=0.1. As would be expected, this two-dimensional theory underpredicts the heating in the three-dimensional stagnation region of the body nose. The theory also underpredicts the laminar heating in the wing region of the body where the complex three-dimensional flow field is not adequately modeled by the theory.

Figure 5 is a summary plot of figure 4 to show more clearly the increase in laminar heating on the bottom centerline of the body with increasing angle of attack. The data from figure 4 for Reynolds numbers between 1×10^6 and 4×10^6 are plotted in figure 5 for $\alpha=15^\circ$, 30°, and 53°. The data are laminar except for the last body station at $\alpha=53^\circ$ where, as previously shown in figure 4, Reynolds-number effects typical of boundary-layer transition occurred.

To further illustrate the effect of angle of attack on the body boundary-layer transition and heating, heating rates for the bottom centerline of the body are plotted in figure 6 for $\alpha=15^\circ$, 20°, 25°, and 30° at a nominal Reynolds number of 7×10^6. For each angle of attack, the increase in heating which starts between x/L=0.5 and 0.6 is characteristic of the beginning of boundary-layer transition. The combination of angle of attack and body boattail, starting at about x/L=0.8, have a pronounced effect on the boundary-layer transition. The heating data for all x/L locations indicate an orderly trend of increased heating with increased angle of attack, except for x/L greater than 0.6 at $\alpha=25^\circ$. The anomaly at $\alpha=25^\circ$ is not fully understood.

Reference 3 includes further discussion of the transition results from this study and their comparison with various transition criteria proposed for space shuttle design.

Top Centerline.- Previous tests (see ref. 4) indicate that complex three dimensional flow fields, containing separation regions and vorticies, occur over the leeward surfaces of the vehicle at angle of attack. These flow fields which are particularly sensitive to angle of attack and Reynolds number, can induce significant effects on leeward heating, as the following data will indicate.

The effects of angle of attack and Reynolds number on leeward heating for the top centerline of the body are shown in figure 7. Of particular interest are the relatively high heating ($\dot{q}_w/\dot{q}_s \approx .04$) near the nose for

$\alpha = 15^{\circ}$, the relatively large increases in heating at the canopy for $\alpha = 15^{\circ}$ and 30°, the minimal increase in canopy heating for $\alpha = 53^{\circ}$, and the overall effect of Reynolds number variation on the top-centerline heating. At $\alpha = 15^{\circ}$, the highest heating in the nose region occurs at the lowest Reynolds number probably because an increase in Reynolds number enables the flow to expand further around the nose before it separates. The increases in canopy heating at $\alpha = 15^{\circ}$ and 30° are caused by the separation vorticies impinging on the canopy, while the minimal increase in canopy heating at $\alpha = 53^{\circ}$ is probably caused by flow separation. The increases in the magnitude of the heating with increasing Reynolds number occur in regions of vortex impingement. This occurs at the canopy and behind it for $\alpha = 15^{\circ}$, in the nose region and at the canopy for $\alpha = 30^{\circ}$, and in the nose region for $\alpha = 53^{\circ}$. Thus the vortex influence on heating decreases with increasing angle of attack. For $\alpha = 30^{\circ}$ and 53°, the heating is low behind the canopy, where the flow is separated, and no substantial changes occur with increasing Reynolds number. However, there are some indications, particularly at $\alpha = 53^{\circ}$, of decreases in heating with increasing Reynolds number.

Side ($\phi \approx 100^{\circ}$). - The effect of sideslip angle, β, on the body side heating for $\alpha = 15^{\circ}$, 30°, and 53° is shown in figure 8 for nominal Reynolds numbers of 1×10^6 and 4×10^6. Heating-rate data for the thermocouples located along the left side (windward for $\beta = -5^{\circ}$) at a body circumferential angle, ϕ, of approximately 100° (see table I and fig. 3) are plotted verses x/L. There is a significant increase in the side heating for the sideslip increase from 0° to 5°, except for the region above the wing at $\alpha = 53^{\circ}$ which, as shown in reference 4, is in separated flow. For the given test conditions, the effects of changes in angle of attack on the side heating forward of the wing, where the flow is attached, are insignificant for both $\beta = 0^{\circ}$ and -5°. However, the side heating above the wing decreases with increasing angle of attack for both $\beta = 0^{\circ}$ and -5° because the side at this station is shielded more from the flow by the wing at higher angles of attack. Also, there are no significant effects of Reynolds number on the side heating, except for above the wing at $\alpha = 15^{\circ}$ and 30°. At $\alpha = 15^{\circ}$ and 30°, the flow separates on top of the wing and impinges along the body side (see ref. 4). With increasing sideslip, the extent of the flow impingement along the side increases and the side heating increases with increasing Reynolds number.

Cross sections. - Heating distributions for body cross sections at x/L=0.2, 0.4, and 0.6 are plotted in figure 9 for $\beta = 0^{\circ}$ and $\alpha = 15^{\circ}$, 30°, and 53° at a nominal Reynolds number of 1×10^6. The data are plotted versus ϕ around the body from the bottom centerline ($\phi = 0^{\circ}$) to the top centerline ($\phi = 180^{\circ}$). Two of the cross sections (at x/L = 0.2 and 0.4) are forward of the wing, while the third one (at x/L = 0.6) is just aft of the wing-body juncture. The differences between the high heating rates for the windward surface and the relatively low heating rates for the side and leeward surfaces are evident from this figure. Also apparent at

$x/L = 0.6$ is the chine heating which is significantly higher than the corresponding bottom-centerline heating. As was also shown in figure 8, the side heating ($\phi \approx 100^{\circ}$) forward of the wing ($x/L = 0.2$ and 0.4) is relatively unaffected by angle-of-attack changes, while above the wing ($x/L = 0.6$) it decreases with increasing angle of attack. In addition, at $\alpha = 15^{\circ}$, the bottom-centerline and side heating rates have comparable magnitudes.

Wing

Wing heating data for the bottom and top surfaces are presented in figures 10 to 14 and 15 to 17, respectively.

Bottom surface.- Chordwise heating distributions on the wing bottom surface for $\alpha = 15^{\circ}$, 30°, and 53° are given in figures 10, 11, and 12, respectively, for three semispan locations. The heating is highest over the leading-edge region of the wing, except for the areas with apparent Reynolds number effects at $\alpha = 15^{\circ}$ and 53°. At these two angles of attack, there are areas where the heating increases with increasing Reynolds number, thus indicating the possibility of boundary-layer transition and/or the effects of the complex flow over the wing with wing-body shock interactions. Reynolds-number effects on the heating were also apparent on the body centerline at these two angles of attack. At $\alpha = 30^{\circ}$, the effect of Reynolds-number variation on the heating-rate ratios is negligible, indicating that the flow was probably laminar. However, it was previously shown that at the highest Reynolds number, 7.24×10^{6}, boundary-layer transition occurred on the body centerline for this angle of attack. Therefore, at this angle of attack, boundary-layer transition apparently did not occur uniformly across the bottom surface. For all three angles of attack, the laminar heating rates for 40-percent chord and aft have about the same magnitude as those along the body centerline in the wing region from $x/L = 0.5$ to 1.0.

Spanwise heating distributions on the wing bottom surface for a nominal Reynolds number of 1×10^{6} are given in figure 13 for $\alpha = 15^{\circ}$, 30°, and 53°. The high levels and significant spanwise variations of the wing heating in the leading-edge region are quite apparent. These give some indications of the complex flow over the wing. Additional measurements would be required to show the detailed spanwise variations in the heating for various chord locations. As was also shown in figures 10 to 12, the heating levels for 40 and 80 percent chord have about the same magnitude as those along the body centerline in the wing region.

The effects of elevon deflections on the wing bottom-surface heating are shown in figure 14 for $\alpha = 15^{\circ}$ and 30°. Deflecting the elevons into the flow causes marked increases in the heating on the elevons. The laminar and turbulent estimates of the elevon heating

rate for fully-attached flows assuming wedge properties at the boundary-layer edge are also presented in figure 14. The wedge angle was taken as the inclination angle of the local surface relative to the free-stream direction, and for the turbulent estimates, the flow was assumed to be turbulent from the wing leading edge. At $\alpha = 15^{\circ}$ and for no elevon deflection, the heating data at the highest Reynolds number, 6×10^6, suggest that the flow becomes turbulent ahead of the elevon. Additional evidence of this is the absence of a separation region ahead of the deflected elevon for the oil-flow patterns of reference 4 at this high Reynolds number. For both $\alpha = 15^{\circ}$ and 30°, the data for the deflected elevons at the lower Reynolds numbers lie above the attached laminar estimates and can, with increasing Reynolds number, approach or exceed the estimated turbulent levels, even though the data for the undeflected elevons are not turbulent. These effects are probably caused by flow separation ahead of the deflected elevon with reattachment near the measurement station and/or by streamwise vorticies on the wing surface (see ref. 4).

Top surfaces.- Chordwise heating distirbutions on the wing top surface for $\alpha = 15^{\circ}$, 30°, and 53° are given in figures 15, 16, and 17; respectively, for four semispan locations. For the three inboard semispan locations at $\alpha = 15^{\circ}$ and 30°, the heating is highest over the leading-edge region of the wing where, as shown in reference 4, the flow is attached. The heating rates decrease further back on the wing where the flow is separated. The large fluctuations in heating at the outboard semispan location are probably caused by flow interference from the wing-tip vertical tail. The separation line on top of the wing moves toward the leading edge with increasing angle of attack until the flow separates at the leading edge (see ref. 4). At $\alpha = 53^{\circ}$, the relatively low heating levels for the top of the wing suggest that the flow separated at the leading edge. The high heating for the two inboard semispan locations at high Reynolds number might be caused by viscous interactions along the wing-body juncture (see ref. 13). At this high angle of attack, interference effects from the vertical tails on the wing heating are minimal compared to those at the lower angles of attack. The complex flow fields over the wing are not fully understood and require more study.

Twin vertical tails.- The heating data obtained for the twin vertical tails was limited because only five thermocouples were available. One result that is presented here is the effect of rudder deflection on the rudder heating. Heating data for the outboard surface of the rudder at 70 percent exposed height of the vertical tail are plotted in figure 18 for $\alpha = 15^{\circ}$ and 30°. The given location on the rudder is above the rudder hinge line on the vertical tail (see table I and fig. 3 (c)). Deflecting the rudder outboard into the flow increases the heating on the rudder surface. However, for the given rudder location and test conditions, there is no significant effect of Reynolds number variation on the rudder heating with or without rudder deflections.

CONCLUDING REMARKS

Aerodynamic heating distributions on a space shuttle delta-wing orbiter model were obtained for various angles of attack and Reynolds numbers at a free-stream Mach number of 7.4. For $\alpha = 15^{\circ}$ to 53°, the laminar heating for the bottom centerline of the body forward of the wing, except for the nose stagnation region, were predicted well by modified swept-cylinder theory. Usually, the effect of increasing angle of attack was to increase the heating on the windward surfaces and decrease the heating on the leeward surfaces where flow separation occurred. On the windward surfaces of the body and wing, increasing Reynolds number caused increases in heating on the aft portions of these surfaces, an effect which is believed to indicate boundary-layer transition from laminar to turbulent flow. At some locations on the windward surface of the wings, however, complications of wing-body interference effects apparently also caused the heating to increase with increasing Reynolds number. Similar trends were observed in regions where reattaching flow occurred, such as on the canopy. Increasing sideslip angle (windward) and deflecting control surfaces (elevon and rudder) caused marked increases in heating on the body side and the control surfaces, respectively.

APPENDIX A

NAR 134B DELTA-WING ORBITER

DIMENSIONAL DATA

TABLE A-I.- BODY FOR DELTA-WING ORBITER

MODEL COMPONENT: BODY - B5

GENERAL DESCRIPTION: Basic delta wing fuselage as per NR lines drawing 9992-134B.

Model Scale = 0.006

DRAWING NUMBER: 9992-134B, S-904-4, -7

DIMENSIONS: (in.)	FULL-SCALE	MODEL SCALE
Length	2120.00	12.720
Max. Width	465.00	2.790
Max. Depth	274.00	1.644
Fineness Ratio	5.906	5.906
Area: ft^2		
Max. Cross-Sectional	702.75	0.0253
Planform	DNA	DNA
Wetted	DNA	DNA
Base	DNA	DNA

TABLE A-II.- WING FOR DELTA-WING ORBITER

MODEL COMPONENT: Wing W15

GENERAL DESCRIPTION: Basic delta wing defined by NR lines drawing 9992-134B.

Model Scale = 0.006

DRAWING NUMBER: 9992-134B; S-904-3,-9,-10,-11,-12

DIMENSIONS:	FULL-SCALE	MODEL SCALE
TOTAL DATA		
Area, ft^2		
Planform	5740.	0.2066
Wetted		
Span (equivalent), in.	1084.00	6.504
Aspect Ratio	1.420	1.420
Rate of Taper	1.719	1.719
Taper Ratio	0.238	0.238
Dihedral Angle, degrees	7.0	7.0
Incidence Angle, degrees	0.0	0.0
Aerodynamic Twist, degrees (About T.E.)	-5.0	-5.0
Incidence, Root (B.P. 240.00)	0.0	0.0
Incidence, Tip (B.P. 542.00)	-5.0	-5.0
Sweep Back Angles, degrees		
Leading Edge	60.0	60.0
Trailing Edge	0.0	0.0
0.25 Element Line	52.20	52.20
Chords: in.		
Root (Wing Sta. 0.0)	1231.77	7.391
Tip, (equivalent)(W.S. 546.07)	293.00	1.758
MAC (W.S. 217.00)	858.72	5.152
Fus. Sta. of .25 MAC	1475.97	8.856
W.P. of .25 MAC	45.90	0.275
B.L. of .25 MAC	215.38	1.292
Airfoil Section		
Root (W.S. 241.80)	NACA 0009-64	
Tip (W.S. 546.06)	NACA 0012-64	
EXPOSED DATA		
Area, ft^2	2377.19	0.08558
Span, (equivalent), in.	613.00	3.678
Aspect Ratio	1.090	1.090
Taper Ratio	0.356	0.356
Chords: in.		
Root (Wing Sta. 237.27)	823.37	4.043
Tip (W.S. 546.07)	293.00	1.758
MAC (W.S. 367.21)	600.49	3.603
Fus. Sta. of .25 MAC	1669.63	10.018
W.P. of .25 MAC	64.20	0.385
B.L. of .25 MAC	364.47	2.187
Leading Edge Cuff		
Planform Area, ft^2	71.44	0.002572
L.E. Intersects Fus. ML at Sta., in.	1061.67	6.370
L.E. Intersects Wing ML at Sta., in.	1407.84	8.447

TABLE A-III.- ELEVON FOR DELTA-WING ORBITER

MODEL COMPONENT: Elevon - E_5

GENERAL DESCRIPTION: Elevon used on W_{15} of delta wing orbiter as per NR 9992-134B lines drawing.

MODEL SCALE = 0.006

DRAWING NUMBER: 9992-134B; S-904-11, -12

DIMENSIONS:	FULL-SCALE	MODEL SCALE
Area, ft^2	432.22	0.01556
Span (equivalent), in.	308.35	1.850
Inb'd equivalent chord, in. (W.S. 218.72)	251.57	1.509
Outb'd equivalent chord, in. (W.S. 527.07)	152.13	0.913
Ratio movable surface chord/ total surface chord		
At Inb'd equiv. chord	0.294	0.294
At Outb'd equiv. chord	0.467	0.467
Sweep Back Angles, degrees		
Leading Edge	17.874	17.874
Tailing Edge	0.0	0.0
Hingeline	17.874	17.874
Area Moment (Normal to hinge line), ft^3	7604.889	0.00162

TABLE A-IV.- VERTICAL TAIL FOR DELTA-WING ORBITER

MODEL COMPONENT: Vertical Tail - V15

GENERAL DESCRIPTION: Twin vertical tail panels of delta wing orbiter. The panels are attached to wing W15. Basic geometry is defined by NR lines drawing 9992-134B.

MODEL SCALE = 0.006

DRAWING NUMBER: 9992-134B; S-904-21, -25

DIMENSIONS:	FULL-SCALE	MODEL SCALE
TOTAL DATA (Data for 1 of 2 sides in vertical tail reference plane)		
Area, ft^2		
Planform	423.01	0.01523
Wetted	-	-
Span (equivalent), in.	303.23	1.819
Aspect Ratio	1.509	1.509
Rate of Taper	0.883	0.883
Taper Ratio	0.200	0.200
Diehedral Angle, degrees	-	-
Incidence Angle, degrees	-	-
Aerodynamic Twist, degrees	-	-
Toe-In Angle, degrees	-1.817	-1.817
Cant Angle, (Top Outb'd), degrees	20.000	20.000
Sweep Back Angles, degrees		
Leading Edge	38.909	38.909
Trailing Edge	-4.700	-4.700
0.25 Element Line	30.252	30.252
Chords: in.		
Root (W.P. 77.23)	334.70	2.008
Tip, (equivalent)(W.P. 362.30)	67.09	0.403
MAC (W.P. 188.12)	230.60	1.384
Fus. Sta. of .25 MAC	1999.21	11.995
W.P. of .25 MAC	188.12	1.129
B.L. of .25 MAC	582.86	3.497
Airfoil Section		
Root	NACA 0012-64	
Tip	NACA 0012-64	
EXPOSED DATA		
Area		
Span, (equivalent)		
Aspect Ratio		
Taper Ratio		
Chords		
Root		
Tip		
MAC		
Fus. Sta. of .25 MAC		
W.P. of .25 MAC		
B.L. of .25 MAC		

TABLE A-V.- RUDDER FOR DELTA-WING ORBITER

MODEL COMPONENT: Rudder R5

GENERAL DESCRIPTION: Rudder used on V15 of delta wing orbiter as per NR 9992-134B lines drawing.

Model Scale = 0.006

DRAWING NUMBER: 9992-134B; S-904-21, -25

DIMENSIONS: (Data for 1 of 2 sides)	FULL-SCALE	MODEL SCALE
Area, ft	292.34	0.01052
Span (equivalent), in.	292.44	1.755
Inb'd equivalent chord, in. (W.P. 87.37)	137.03	0.822
Outb'd equivalent chord (W.P. 362.30)	67.09	0.402
Ratio movable surface chord/ total surface chord		
At Inb'd equiv. chord,	0.421	0.421
At Outb'd equiv. chord,	1.000	1.000
Sweep Back Angles, degrees		
Leading Edge	-	-
Tailing Edge	-	-
Hingeline	-19.701	-19.701
Area Moment (Normal to hinge line)	4006.157	0.0008653
Hingeline Passes Through		
Fus. Sta., in.	2046.89	12.281
B.P., in.	542.00	3.252
W.P., in.	79.60	0.478
and		
Fus. Sta., in.	1985.63	11.914
B.P., in.	602.06	3.612
W.P., in.	239.33	1.439

APPENDIX B

TABULATED HEAT TRANSFER DATA

NAR 134B Delta-Wing Orbiter
NASA-Ames 3.5-ft. HWT
Test 106 Runs 1-16, 18-26, 54-60, and 66

ADDITIONAL NOMENCLATURE FOR APPENDIX B

CHANNEL	recording-system channel
MACH	free-stream Mach number
PT	free-stream total pressure, psia
QS	stagnation-point heat-transfer rate for reference sphere, Btu/ft^2-sec
QW	heat-transfer rate at model wall for given T/C location, Btu/ft^2-sec
QW/QS	heating-rate ratio
REL	free-stream Reynolds number based on model reference length
REYN/FT	free-stream Reynolds number per foot
RSPH	reference sphere radius, 0.183 cm (0.006 ft) for test, equivalent to 0.305 m (1 ft) for full-scale vehicle
T/C	thermocouple number
TEMP	model wall temperature at given T/C location, ^oR
TT	free-stream total temperature, ^oR
TWSPH	reference sphere wall temperature, ^oR

$\alpha = -5^{\circ}$ $\beta = 0^{\circ}$ $\delta_e = 0^{\circ}$ $\delta_r = 0^{\circ}$ TEST NO. 106 RUN NO. 55

MACH	REYN/FT	REL	QS	TWSPH	PT	TT	RSPH(FT)
7.40	7.03E 05	7.50E 05	37.74	550.	158.	1431.	0.006

CHANNEL	T/C	TEMP	QW/QS	CHANNEL	T/C	TEMP	QW/QS
1	1	572.	0.761	41	50	544.	0.011
2	2	565.	0.388	42	51	550.	0.054
3	3	559.	0.230	43	52	548.	0.037
4	4	548.	0.057	44	53	545.	0.016
5	5	558.	0.160	45	54	544.	0.009
6	6	549.	0.116	46	55	543.	0.004
7	7	544.	0.012	47	56	-	-
8	8	545.	0.041	48	57	546.	0.022
9	9	-	-	49	58	545.	0.011
10	10	543.	0.004	50	59	544.	0.006
11	11	545.	0.030	51	60	561.	0.251
12	12	546.	0.053	52	62	545.	0.014
13	13	549.	0.125	53	63	544.	0.007
14	14	555.	0.348	54	64	549.	0.002
15	16	550.	0.073	55	65	544.	0.001
16	17	547.	0.062	56	66	552.	0.080
17	18	543.	0.006	57	67	549.	0.051
18	19	544.	0.021	58	68	547.	0.029
19	20	546.	0.056	59	69	544.	0.009
20	21	544.	0.005	60	70	559.	0.170
21	23	544.	0.008	61	72	548.	0.054
22	24	544.	0.016	62	73	545.	0.020
23	26	544.	0.009	63	74	544.	0.011
24	28	544.	0.011	64	75	544.	0.0
25	32	545.	0.014	65	76	548.	0.055
26	33	545.	0.031	66	77	548.	0.057
27	34	545.	0.017	67	78	549.	0.059
28	35	544.	0.012	68	79	553.	0.079
29	36	546.	0.030	69	80	550.	0.062
30	37	545.	0.015	70	81	547.	0.044
31	38	544.	0.009	71	82	556.	0.130
32	41	545.	0.015	72	84	550.	0.059
33	42	544.	0.004	73	85	546.	0.032
34	43	545.	0.023	74	86	545.	0.014
35	44	544.	0.007	75	87	544.	0.005
36	45	545.	0.020	76	88	560.	0.170
37	46	544.	0.010	77	89	551.	0.085
38	47	543.	0.0	78	90	548.	0.047
39	48	544.	0.005	79	91	567.	0.261
40	49	543.	0.0	80	92	547.	0.036

$\alpha = -5^{\circ}$ $\beta = 0^{\circ}$ $\delta_e = 0^{\circ}$ $\delta_r = 0^{\circ}$ TEST NO. 106 RUN NO. 57

MACH	REYN/FT	REL	QS	TWSPH	PT	TT	RSPH(FT)
7.40	3.50E 06	3.71E 06	78.84	557.	758.	1400.	0.006

CHANNEL	T/C	TEMP	QW/QS	CHANNEL	T/C	TEMP	QW/QS
1	1	603.	0.733	41	50	545.	0.008
2	2	588.	0.366	42	51	556.	0.056
3	3	577.	0.216	43	52	553.	0.043
4	4	553.	0.048	44	53	548.	0.017
5	5	574.	0.152	45	54	547.	0.010
6	6	556.	0.112	46	55	545.	0.005
7	7	545.	0.009	47	56	-	-
8	8	548.	0.038	48	57	550.	0.027
9	9	-	-	49	58	547.	0.012
10	10	544.	0.004	50	59	546.	0.006
11	11	547.	0.028	51	60	580.	0.238
12	12	549.	0.046	52	62	545.	0.011
13	13	563.	0.174	53	63	545.	0.005
14	14	575.	0.473	54	64	549.	0.001
15	16	558.	0.083	55	65	545.	0.001
16	17	-	-	56	66	565.	0.097
17	18	544.	0.012	57	67	561.	0.082
18	19	545.	0.016	58	68	557.	0.058
19	20	552.	0.059	59	69	547.	0.015
20	21	544.	0.003	60	70	575.	0.163
21	23	545.	0.018	61	72	552.	0.047
22	24	545.	0.019	62	73	546.	0.016
23	26	547.	0.020	63	74	545.	0.009
24	28	546.	0.022	64	75	546.	0.0
25	32	545.	0.029	65	76	553.	0.052
26	33	548.	0.039	66	77	553.	0.044
27	34	548.	0.039	67	78	554.	0.052
28	35	545.	0.009	68	79	563.	0.068
29	36	550.	0.044	69	80	564.	0.091
30	37	546.	0.024	70	81	553.	0.052
31	38	545.	0.006	71	82	570.	0.121
32	41	546.	0.019	72	84	557.	0.055
33	42	544.	0.002	73	85	549.	0.029
34	43	547.	0.028	74	86	547.	0.012
35	44	545.	0.005	75	87	546.	0.002
36	45	549.	0.028	76	88	575.	0.152
37	46	545.	0.008	77	89	560.	0.084
38	47	544.	0.001	78	90	556.	0.048
39	48	545.	0.002	79	91	590.	0.225
40	49	545.	0.003	80	92	553.	0.031

$\alpha = 0^{o}$ $\beta = 0^{o}$ $\delta_e = 0^{o}$ $\delta_r = 0^{o}$ TEST NO. 106 RUN NO. 54

MACH	REYN/FT	REL	QS	TWSPH	PT	TT	RSPH(FT)
7.40	6.36E 05	6.70E 05	41.03	558.	157.	1513.	0.006

CHANNEL	T/C	TEMP	QW/QS	CHANNEL	T/C	TEMP	QW/QS
1	1	578.	0.772	41	50	545.	0.008
2	2	568.	0.354	42	51	549.	0.038
3	3	561.	0.191	43	52	548.	0.024
4	4	554.	0.087	44	53	545.	0.011
5	5	559.	0.127	45	54	545.	0.006
6	6	552.	0.088	46	55	544.	0.002
7	7	548.	0.024	47	56	-	-
8	8	549.	0.040	48	57	546.	0.015
9	9	-	-	49	58	545.	0.008
10	10	547.	0.008	50	59	544.	0.004
11	11	548.	0.026	51	60	567.	0.286
12	12	549.	0.036	52	62	546.	0.026
13	13	551.	0.082	53	63	545.	0.013
14	14	557.	0.301	54	64	549.	0.003
15	16	552.	0.055	55	65	544.	0.003
16	17	550.	0.052	56	66	551.	0.063
17	18	547.	0.005	57	67	548.	0.041
18	19	548.	0.020	58	68	547.	0.023
19	20	550.	0.046	59	69	544.	0.009
20	21	548.	0.010	60	70	562.	0.182
21	23	546.	0.004	61	72	550.	0.075
22	24	547.	0.016	62	73	546.	0.030
23	26	547.	0.005	63	74	545.	0.018
24	28	546.	0.005	64	75	545.	0.0
25	32	546.	0.006	65	76	551.	0.076
26	33	548.	0.055	66	77	550.	0.070
27	34	546.	0.016	67	78	552.	0.088
28	35	546.	0.007	68	79	550.	0.054
29	36	546.	0.013	69	80	547.	0.040
30	37	545.	0.006	70	81	546.	0.028
31	38	546.	0.017	71	82	568.	0.169
32	41	545.	0.006	72	84	553.	0.083
33	42	545.	0.009	73	85	548.	0.048
34	43	545.	0.015	74	86	545.	0.023
35	44	545.	0.005	75	87	545.	0.008
36	45	546.	0.016	76	88	560.	0.165
37	46	545.	0.004	77	89	548.	0.055
38	47	544.	0.001	78	90	546.	0.035
39	48	545.	0.003	79	91	566.	0.250
40	49	544.	0.002	80	92	547.	0.038

$\alpha = 0^{o}$ $\beta = 0^{o}$ $\delta_{e} = 0^{o}$ $\delta_{r} = 0^{o}$

TEST NO. 106 RUN NO. 56

MACH	REYN/FT	REL	QS	TWSPH	PT	TT	RSPH(FT)
7.40	3.37E 06	3.57E 06	80.61	565.	754.	1427.	0.006

CHANNEL	T/C	TEMP	QW/QS	CHANNEL	T/C	TEMP	QW/QS
1	1	608.	0.775	41	50	548.	0.007
2	2	584.	0.333	42	51	555.	0.035
3	3	572.	0.178	43	52	552.	0.025
4	4	559.	0.074	44	53	550.	0.010
5	5	568.	0.117	45	54	548.	0.006
6	6	555.	0.082	46	55	547.	0.002
7	7	548.	0.018	47	56	-	-
8	8	549.	0.036	48	57	551.	0.015
9	9	-	-	49	58	549.	0.006
10	10	547.	0.005	50	59	547.	0.003
11	11	549.	0.025	51	60	588.	0.265
12	12	549.	0.028	52	62	549.	0.020
13	13	561.	0.138	53	63	548.	0.009
14	14	572.	0.382	54	64	552.	0.002
15	16	558.	0.064	55	65	547.	0.002
16	17	553.	0.056	56	66	560.	0.057
17	18	547.	0.004	57	67	556.	0.037
18	19	548.	0.017	58	68	553.	0.022
19	20	557.	0.058	59	69	548.	0.005
20	21	548.	0.007	60	70	578.	0.169
21	23	548.	0.009	61	72	557.	0.057
22	24	548.	0.015	62	73	551.	0.030
23	26	549.	0.005	63	74	549.	0.018
24	28	548.	0.012	64	75	548.	0.003
25	32	549.	0.015	65	76	556.	0.061
26	33	553.	0.054	66	77	557.	0.060
27	34	549.	0.017	67	78	561.	0.079
28	35	549.	0.010	68	79	557.	0.045
29	36	552.	0.027	69	80	558.	0.055
30	37	548.	0.013	70	81	551.	0.026
31	38	549.	0.014	71	82	580.	0.152
32	41	548.	0.012	72	84	563.	0.073
33	42	548.	0.006	73	85	553.	0.042
34	43	549.	0.014	74	86	550.	0.016
35	44	548.	0.005	75	87	548.	0.006
36	45	551.	0.021	76	88	575.	0.137
37	46	548.	0.009	77	89	557.	0.056
38	47	547.	0.001	78	90	553.	0.032
39	48	548.	0.005	79	91	587.	0.207
40	49	548.	0.001	80	92	554.	0.032

$\alpha = 15^{\circ}$ $\beta = 0^{\circ}$ $\delta_e = 0^{\circ}$ $\delta_r = 0^{\circ}$ TEST NO. 106 RUN NO. 1

MACH	REYN/FT	REL	QS	TWSPH	PT	TT	RSPH(FT)
7.40	1.08E 06	1.14E 06	48.54	571.	252.	1466.	0.006

CHANNEL	T/C	TEMP	QW/QS	CHANNEL	T/C	TEMP	QW/QS
1	1	585.	0.856	41	50	543.	0.002
2	2	-	-	42	51	545.	0.013
3	3	-	-	43	52	543.	0.006
4	4	563.	0.192	44	53	543.	0.002
5	5	548.	0.043	45	54	542.	0.002
6	6	-	-	46	55	542.	0.0
7	7	548.	0.074	47	56	544.	0.010
8	8	545.	0.035	48	57	543.	0.003
9	9	544.	0.008	49	58	543.	0.0
10	10	546.	0.036	50	59	542.	0.0
11	11	545.	0.025	51	60	560.	0.339
12	12	544.	0.004	52	62	547.	0.064
13	13	544.	0.006	53	63	545.	0.038
14	14	545.	0.020	54	64	544.	0.022
15	16	545.	0.006	55	65	543.	0.015
16	17	545.	0.013	56	66	545.	0.024
17	18	545.	0.023	57	67	544.	0.013
18	19	545.	0.021	58	68	543.	0.006
19	20	544.	0.006	59	69	542.	0.002
20	21	544.	0.005	60	70	559.	0.151
21	23	545.	0.019	61	72	551.	0.092
22	24	545.	0.018	62	73	547.	0.055
23	26	544.	0.003	63	74	545.	0.034
24	28	545.	0.017	64	75	543.	0.014
25	32	544.	0.019	65	76	553.	0.108
26	33	550.	0.098	66	77	553.	0.107
27	34	544.	0.016	67	78	556.	0.128
28	35	543.	0.001	68	79	544.	0.020
29	36	544.	0.006	69	80	543.	0.015
30	37	544.	0.016	70	81	542.	0.010
31	38	547.	0.044	71	82	566.	0.188
32	41	545.	0.017	72	84	558.	0.119
33	42	545.	0.025	73	85	549.	0.084
34	43	543.	0.006	74	86	545.	0.039
35	44	543.	0.001	75	87	543.	0.017
36	45	543.	0.006	76	88	555.	0.140
37	46	544.	0.009	77	89	542.	0.015
38	47	543.	0.008	78	90	544.	0.040
39	48	544.	0.005	79	91	547.	0.182
40	49	543.	0.006	80	92	545.	0.037

$\alpha = 15^{o}$ $\beta = 0^{o}$ $\delta_e = 0^{o}$ $\delta_r = 0^{o}$ TEST NO. 106 RUN NO. 2

MACH	REYN/FT	REL	QS	TWSPH	PT	TT	RSPH(FT)
7.40	3.66E 06	3.88E 06	105.92	605.	978.	1586.	0.006

CHANNEL	T/C	TEMP	QW/QS	CHANNEL	T/C	TEMP	QW/QS
1	1	605.	0.879	41	50	544.	0.003
2	2	-	-	42	51	-	-
3	3	-	-	43	52	545.	0.004
4	4	586.	0.193	44	53	544.	0.002
5	5	550.	0.041	45	54	544.	0.002
6	6	-	-	46	55	543.	0.0
7	7	550.	0.076	47	56	547.	0.009
8	8	544.	0.035	48	57	544.	0.002
9	9	540.	0.007	49	58	544.	0.001
10	10	547.	0.035	50	59	543.	0.001
11	11	544.	0.026	51	60	584.	0.334
12	12	541.	0.005	52	62	553.	0.060
13	13	542.	0.009	53	63	550.	0.040
14	14	546.	0.035	54	64	547.	0.026
15	16	543.	0.012	55	65	546.	0.018
16	17	544.	0.020	56	66	550.	0.026
17	18	544.	0.024	57	67	547.	0.015
18	19	544.	0.022	58	68	545.	0.008
19	20	543.	0.010	59	69	543.	0.002
20	21	544.	0.009	60	70	585.	0.154
21	23	544.	0.024	61	72	565.	0.094
22	24	543.	0.019	62	73	551.	0.052
23	26	545.	0.010	63	74	549.	0.029
24	28	545.	0.023	64	75	546.	0.015
25	32	545.	0.026	65	76	569.	0.113
26	33	559.	0.101	66	77	568.	0.109
27	34	544.	0.017	67	78	575.	0.126
28	35	543.	0.001	68	79	549.	0.024
29	36	545.	0.011	69	80	552.	0.030
30	37	546.	0.023	70	81	545.	0.011
31	38	550.	0.045	71	82	601.	0.185
32	41	547.	0.020	72	84	580.	0.119
33	42	548.	0.025	73	85	560.	0.079
34	43	545.	0.009	74	86	550.	0.040
35	44	544.	0.002	75	87	546.	0.013
36	45	546.	0.009	76	88	575.	0.136
37	46	545.	0.012	77	89	545.	0.015
38	47	544.	0.013	78	90	551.	0.042
39	48	544.	0.005	79	91	556.	0.176
40	49	546.	0.007	80	92	552.	0.039

$\alpha = 15^{\circ}$ $\beta = 0^{\circ}$ $\delta_e = 0^{\circ}$ $\delta_r = 0^{\circ}$ TEST NO. 106 RUN NO. 18

MACH	REYN/FT	REL	QS	TWSPH	PT	TT	RSPH(FT)
7.40	5.86E 06	6.21E 06	115.05	622.	1436.	1507.	0.006

CHANNEL	T/C	TEMP	QW/QS	CHANNEL	T/C	TEMP	QW/QS
1	1	616.	0.922	41	50	553.	0.003
2	2	-	-	42	51	555.	0.010
3	3	-	-	43	52	554.	0.004
4	4	601.	0.198	44	53	552.	0.002
5	5	563.	0.038	45	54	553.	0.002
6	6	-	-	46	55	552.	0.0
7	7	562.	0.079	47	56	555.	0.009
8	8	556.	0.035	48	57	553.	0.003
9	9	552.	0.006	49	58	552.	0.002
10	10	559.	0.035	50	59	552.	0.001
11	11	555.	0.026	51	60	597.	0.354
12	12	553.	0.008	52	62	565.	0.071
13	13	554.	0.008	53	63	567.	0.076
14	14	561.	0.046	54	64	565.	0.082
15	16	555.	0.011	55	65	563.	0.050
16	17	556.	0.023	56	66	560.	0.027
17	18	556.	0.022	57	67	557.	0.016
18	19	555.	0.023	58	68	555.	0.008
19	20	555.	0.011	59	69	552.	0.002
20	21	555.	0.010	60	70	598.	0.175
21	23	555.	0.017	61	72	578.	0.099
22	24	554.	0.020	62	73	563.	0.049
23	26	556.	0.014	63	74	560.	0.031
24	28	555.	0.015	64	75	564.	0.046
25	32	554.	0.019	65	76	582.	0.120
26	33	571.	0.108	66	77	581.	0.115
27	34	554.	0.018	67	78	589.	0.130
28	35	552.	0.001	68	79	560.	0.023
29	36	555.	0.012	69	80	563.	0.031
30	37	-	-	70	81	554.	0.007
31	38	561.	0.046	71	82	618.	0.197
32	41	569.	0.107	72	84	597.	0.126
33	42	559.	0.028	73	85	576.	0.092
34	43	554.	0.010	74	86	566.	0.067
35	44	553.	0.003	75	87	562.	0.039
36	45	555.	0.009	76	88	587.	0.134
37	46	560.	0.051	77	89	555.	0.015
38	47	554.	0.017	78	90	563.	0.042
39	48	558.	0.024	79	91	598.	0.179
40	49	559.	0.025	80	92	565.	0.041

$\alpha = 15^{\circ}$ $\beta = 0^{\circ}$ $\delta_e = 0^{\circ}$ $\delta_r = 0^{\circ}$ TEST NO. 106 RUN NO. 60

MACH	REYN/FT	REL	QS	TWSPH	PT	TT	RSPH(FT)
7.40	6.92E 06	7.34E 06	103.26	604.	1486.	1394.	0.006

CHANNEL	T/C	TEMP	QW/QS	CHANNEL	T/C	TEMP	QW/QS
1	1	616.	0.861	41	50	553.	0.003
2	2	-	-	42	51	554.	0.009
3	3	-	-	43	52	553.	0.003
4	4	586.	0.193	44	53	553.	0.002
5	5	558.	0.035	45	54	553.	0.002
6	6	-	-	46	55	552.	0.001
7	7	557.	0.074	47	56	-	-
8	8	553.	0.033	48	57	553.	0.002
9	9	-	-	49	58	552.	0.001
10	10	555.	0.034	50	59	552.	0.001
11	11	553.	0.026	51	60	580.	0.355
12	12	550.	0.010	52	62	562.	0.070
13	13	552.	0.012	53	63	564.	0.074
14	14	557.	0.044	54	64	558.	0.063
15	16	552.	0.010	55	65	559.	0.046
16	17	553.	0.023	56	66	558.	0.024
17	18	553.	0.020	57	67	555.	0.013
18	19	553.	0.022	58	68	554.	0.006
19	20	553.	0.013	59	69	552.	0.001
20	21	553.	0.011	60	70	610.	0.164
21	23	553.	0.015	61	72	573.	0.092
22	24	-	-	62	73	560.	0.054
23	26	554.	0.012	63	74	562.	0.080
24	28	553.	0.013	64	75	560.	0.037
25	32	554.	0.016	65	76	575.	0.113
26	33	565.	0.106	66	77	574.	0.110
27	34	554.	0.021	67	78	580.	0.122
28	35	552.	0.001	68	79	556.	0.015
29	36	554.	0.012	69	80	555.	0.014
30	37	556.	0.030	70	81	554.	0.014
31	38	559.	0.045	71	82	597.	0.194
32	41	560.	0.062	72	84	583.	0.118
33	42	557.	0.026	73	85	570.	0.091
34	43	554.	0.011	74	86	569.	0.124
35	44	553.	0.002	75	87	560.	0.044
36	45	554.	0.009	76	88	576.	0.126
37	46	557.	0.043	77	89	554.	0.013
38	47	554.	0.019	78	90	559.	0.043
39	48	556.	0.022	79	91	585.	0.164
40	49	555.	0.007	80	92	561.	0.040

$\alpha = 15^{\circ}$ $\beta = 0^{\circ}$ $\delta_e = +14^{\circ}$ $\delta_r = \pm 20^{\circ}$ TEST NO. 106 RUN NO. 19

MACH	REYN/FT	REL	QS	TWSPH	PT	TT	RSPH(FT)
7.40	8.04E 05	8.50E 05	56.68	582.	232.	1655.	0.006

CHANNEL	T/C	TEMP	QW/QS	CHANNEL	T/C	TEMP	QW/QS
1	1	588.	0.912	41	50	558.	0.003
2	2	-	-	42	51	558.	0.012
3	3	-	-	43	52	557.	0.006
4	4	572.	0.187	44	53	557.	0.002
5	5	559.	0.041	45	54	557.	0.001
6	6	-	-	46	55	556.	0.0
7	7	557.	0.073	47	56	558.	0.011
8	8	555.	0.032	48	57	557.	0.004
9	9	554.	0.008	49	58	557.	0.002
10	10	557.	0.037	50	59	556.	0.0
11	11	555.	0.025	51	60	577.	0.344
12	12	554.	0.003	52	62	560.	0.063
13	13	554.	0.006	53	63	558.	0.036
14	14	556.	0.022	54	64	557.	0.023
15	16	555.	0.006	55	65	560.	0.057
16	17	555.	0.014	56	66	560.	0.025
17	18	556.	0.023	57	67	558.	0.013
18	19	556.	0.022	58	68	558.	0.006
19	20	556.	0.007	59	69	-	-
20	21	556.	0.006	60	70	585.	0.163
21	23	556.	0.019	61	72	566.	0.085
22	24	556.	0.019	62	73	560.	0.052
23	26	557.	0.003	63	74	559.	0.033
24	28	556.	0.016	64	75	561.	0.051
25	32	557.	0.017	65	76	566.	0.105
26	33	562.	0.100	66	77	565.	0.101
27	34	557.	0.016	67	78	570.	0.124
28	35	557.	0.001	68	79	558.	0.019
29	36	557.	0.007	69	80	557.	0.010
30	37	557.	0.017	70	81	556.	0.002
31	38	559.	0.044	71	82	578.	0.197
32	41	557.	0.015	72	84	570.	0.117
33	42	558.	0.025	73	85	562.	0.076
34	43	557.	0.006	74	86	559.	0.038
35	44	557.	0.001	75	87	560.	0.050
36	45	558.	0.007	76	88	568.	0.130
37	46	557.	0.008	77	89	556.	0.016
38	47	556.	0.011	78	90	555.	0.006
39	48	557.	0.006	79	91	579.	0.230
40	49	558.	0.006	80	92	565.	0.090

$\alpha = 15^{\circ}$ $\beta = 0^{\circ}$ $\delta_e = +14^{\circ}$ $\delta_r = \pm 20^{\circ}$ TEST NO. 106 RUN NO. 20

MACH	REYN/FT	REL	QS	TWSPH	PT	TT	RSPH(FT)
7.40	3.75E 06	3.98E 06	99.68	608.	958.	1544.	0.006

CHANNEL	T/C	TEMP	QW/QS	CHANNEL	T/C	TEMP	QW/QS
1	1	621.	0.877	41	50	558.	0.002
2	2	-	-	42	51	-	-
3	3	-	-	43	52	558.	0.004
4	4	590.	0.191	44	53	557.	0.002
5	5	563.	0.038	45	54	557.	0.002
6	6	-	-	46	55	556.	0.0
7	7	563.	0.073	47	56	559.	0.009
8	8	559.	0.033	48	57	558.	0.003
9	9	556.	0.007	49	58	557.	0.001
10	10	561.	0.034	50	59	556.	0.001
11	11	558.	0.024	51	60	599.	0.343
12	12	556.	0.004	52	62	565.	0.062
13	13	557.	0.008	53	63	564.	0.039
14	14	561.	0.035	54	64	561.	0.033
15	16	558.	0.010	55	65	576.	0.105
16	17	559.	0.020	56	66	562.	0.026
17	18	559.	0.021	57	67	560.	0.014
18	19	559.	0.022	58	68	559.	0.007
19	20	557.	0.009	59	69	557.	0.001
20	21	558.	0.009	60	70	612.	0.165
21	23	559.	0.016	61	72	574.	0.090
22	24	558.	0.018	62	73	564.	0.054
23	26	558.	0.009	63	74	561.	0.030
24	28	559.	0.014	64	75	580.	0.133
25	32	559.	0.017	65	76	577.	0.113
26	33	571.	0.105	66	77	577.	0.104
27	34	559.	0.017	67	78	582.	0.125
28	35	557.	0.001	68	79	562.	0.021
29	36	559.	0.011	69	80	564.	0.025
30	37	560.	0.016	70	81	557.	0.002
31	38	564.	0.045	71	82	598.	0.198
32	41	561.	0.019	72	84	586.	0.119
33	42	562.	0.026	73	85	570.	0.080
34	43	558.	0.009	74	86	563.	0.040
35	44	557.	0.001	75	87	572.	0.094
36	45	559.	0.008	76	88	580.	0.128
37	46	560.	0.012	77	89	558.	0.012
38	47	558.	0.011	78	90	556.	0.002
39	48	559.	0.006	79	91	600.	0.220
40	49	560.	0.007	80	92	577.	0.098

$\alpha = 15^{\circ}$ $\beta = -5^{\circ}$ $\delta_e = +14^{\circ}$ $\delta_r = \pm 20^{\circ}$ TEST NO. 106 RUN NO. 21

MACH	REYN/FT	REL	QS	TWSPH	PT	TT	RSPH(FT)
7.40	1.03E 06	1.09E 06	50.08	578.	250.	1502.	0.006

CHANNEL	T/C	TEMP	QW/QS	CHANNEL	T/C	TEMP	QW/QS
1	1	591.	0.863	41	50	550.	0.002
2	2	-	-	42	51	551.	0.007
3	3	-	-	43	52	550.	0.004
4	4	569.	0.191	44	53	550.	0.0
5	5	555.	0.042	45	54	550.	0.0
6	6	-	-	46	55	551.	0.0
7	7	554.	0.076	47	56	551.	0.004
8	8	552.	0.052	48	57	551.	0.003
9	9	550.	0.007	49	58	550.	0.0
10	10	553.	0.038	50	59	551.	0.0
11	11	552.	0.039	51	60	573.	0.400
12	12	549.	0.003	52	62	555.	0.067
13	13	550.	0.006	53	63	553.	0.038
14	14	553.	0.052	54	64	552.	0.024
15	16	552.	0.019	55	65	558.	0.065
16	17	551.	0.027	56	66	553.	0.020
17	18	551.	0.028	57	67	552.	0.010
18	19	552.	0.034	58	68	551.	0.004
19	20	551.	0.014	59	69	551.	0.0
20	21	551.	0.006	60	70	576.	0.194
21	23	551.	0.026	61	72	565.	0.115
22	24	552.	0.029	62	73	555.	0.063
23	26	551.	0.003	63	74	554.	0.040
24	28	551.	0.024	64	75	557.	0.040
25	32	551.	0.026	65	76	565.	0.129
26	33	559.	0.124	66	77	565.	0.122
27	34	552.	0.028	67	78	570.	0.152
28	35	550.	0.002	68	79	553.	0.020
29	36	550.	0.004	69	80	552.	0.010
30	37	551.	0.025	70	81	551.	0.002
31	38	554.	0.053	71	82	589.	0.231
32	41	551.	0.022	72	84	574.	0.142
33	42	553.	0.032	73	85	561.	0.091
34	43	552.	0.019	74	86	556.	0.046
35	44	550.	0.001	75	87	556.	0.036
36	45	551.	0.004	76	88	572.	0.129
37	46	551.	0.012	77	89	553.	0.028
38	47	550.	0.012	78	90	552.	0.007
39	48	550.	0.006	79	91	587.	0.230
40	49	552.	0.010	80	92	567.	0.091

$\alpha = 15^{\circ}$ $\beta = -5^{\circ}$ $\delta_e = +14^{\circ}$ $\delta_r = \pm 20^{\circ}$ TEST NO. 106 RUN NO. 22

MACH	REYN/FT	REL	QS	TWSPH	PT	TT	RSPH(FT)
7.40	4.10E 06	4.35E 06	94.20	603.	977.	1483.	0.006

CHANNEL	T/C	TEMP	QW/QS	CHANNEL	T/C	TEMP	QW/QS
1	1	626.	0.841	41	50	556.	0.002
2	2	-	-	42	51	556.	0.004
3	3	-	-	43	52	556.	0.002
4	4	586.	0.188	44	53	555.	0.0
5	5	559.	0.037	45	54	555.	0.0
6	6	-	-	46	55	554.	0.0
7	7	558.	0.075	47	56	556.	0.004
8	8	556.	0.051	48	57	555.	0.001
9	9	550.	0.006	49	58	555.	0.0
10	10	556.	0.038	50	59	554.	0.0
11	11	555.	0.038	51	60	597.	0.401
12	12	550.	0.002	52	62	564.	0.073
13	13	551.	0.006	53	63	559.	0.043
14	14	563.	0.080	54	64	556.	0.027
15	16	557.	0.029	55	65	585.	0.176
16	17	554.	0.028	56	66	559.	0.019
17	18	555.	0.028	57	67	557.	0.011
18	19	556.	0.033	58	68	556.	0.006
19	20	558.	0.023	59	69	554.	0.0
20	21	555.	0.004	60	70	602.	0.198
21	23	555.	0.025	61	72	582.	0.118
22	24	555.	0.027	62	73	564.	0.064
23	26	555.	0.003	63	74	562.	0.039
24	28	555.	0.024	64	75	585.	0.162
25	32	555.	0.029	65	76	583.	0.129
26	33	571.	0.125	66	77	579.	0.121
27	34	556.	0.033	67	78	591.	0.146
28	35	555.	0.002	68	79	560.	0.025
29	36	556.	0.004	69	80	561.	0.026
30	37	555.	0.025	70	81	555.	0.002
31	38	561.	0.054	71	82	626.	0.220
32	41	556.	0.024	72	84	596.	0.142
33	42	559.	0.043	73	85	577.	0.098
34	43	560.	0.030	74	86	563.	0.049
35	44	555.	0.002	75	87	580.	0.135
36	45	556.	0.005	76	88	593.	0.123
37	46	554.	0.014	77	89	559.	0.022
38	47	553.	0.015	78	90	555.	0.002
39	48	553.	0.006	79	91	617.	0.226
40	49	558.	0.014	80	92	584.	0.097

$\alpha = 20^{o}$ $\beta = 0^{o}$ $\delta_e = 0^{o}$ $\delta_r = 0^{o}$ TEST NO. 106 RUN NO. 59

MACH	REYN/FT	REL	QS	TWSPH	PT	TT	RSPH(FT)
7.40	6.82E 06	7.23E 06	102.46	624.	1487.	1406.	0.006

CHANNEL	T/C	TEMP	QW/QS	CHANNEL	T/C	TEMP	QW/QS
1	1	642.	0.806	41	50	551.	0.002
2	2	-	-	42	51	552.	0.006
3	3	-	-	43	52	551.	0.002
4	4	602.	0.238	44	53	551.	0.002
5	5	555.	0.026	45	54	551.	0.002
6	6	-	-	46	55	550.	0.0
7	7	561.	0.101	47	56	-	-
8	8	552.	0.036	48	57	551.	0.001
9	9	-	-	49	58	551.	0.001
10	10	558.	0.050	50	59	550.	0.001
11	11	552.	0.027	51	60	593.	0.351
12	12	553.	0.028	52	62	566.	0.081
13	13	558.	0.052	53	63	565.	0.070
14	14	558.	0.105	54	64	558.	0.052
15	16	551.	0.012	55	65	559.	0.037
16	17	552.	0.024	56	66	554.	0.017
17	18	554.	0.033	57	67	553.	0.010
18	19	552.	0.023	58	68	552.	0.005
19	20	550.	0.006	59	69	550.	0.001
20	21	550.	0.006	60	70	594.	0.165
21	23	554.	0.024	61	72	579.	0.118
22	24	552.	0.011	62	73	565.	0.072
23	26	552.	0.007	63	74	562.	0.058
24	28	555.	0.023	64	75	565.	0.077
25	32	555.	0.029	65	76	582.	0.134
26	33	569.	0.119	66	77	582.	0.132
27	34	552.	0.017	67	78	588.	0.143
28	35	550.	0.001	68	79	553.	0.012
29	36	552.	0.008	69	80	553.	0.011
30	37	556.	0.045	70	81	551.	0.004
31	38	562.	0.056	71	82	609.	0.189
32	41	558.	0.088	72	84	595.	0.135
33	42	559.	0.033	73	85	572.	0.101
34	43	551.	0.008	74	86	561.	0.054
35	44	551.	0.004	75	87	563.	0.066
36	45	552.	0.006	76	88	577.	0.122
37	46	555.	0.066	77	89	552.	0.008
38	47	556.	0.032	78	90	555.	0.022
39	48	555.	0.036	79	91	586.	0.177
40	49	555.	0.012	80	92	560.	0.038

$\alpha = 25^{\circ}$ $\beta = 0^{\circ}$ $\delta_e = 0^{\circ}$ $\delta_r = 0^{\circ}$ TEST NO. 106 RUN NO. 66

MACH	REYN/FT	REL	QS	TWSPH	PT	TT	RSPH(FT)
7.40	6.61E 06	7.00E 06	105.94	638.	1501.	1440.	0.006

CHANNEL	T/C	TEMP	QW/QS	CHANNEL	T/C	TEMP	QW/QS
1	1	640.	0.812	41	50	552.	0.003
2	2	-	-	42	51	552.	0.004
3	3	-	-	43	52	551.	0.002
4	4	611.	0.283	44	53	551.	0.003
5	5	551.	0.019	45	54	551.	0.003
6	6	-	-	46	55	550.	0.0
7	7	562.	0.128	47	56	-	-
8	8	550.	0.034	48	57	551.	0.001
9	9	547.	0.014	49	58	551.	0.002
10	10	559.	0.069	50	59	551.	0.004
11	11	550.	0.025	51	60	587.	0.322
12	12	550.	0.025	52	62	565.	0.092
13	13	551.	0.052	53	63	563.	0.087
14	14	553.	0.080	54	64	557.	0.095
15	16	549.	0.008	55	65	567.	0.100
16	17	550.	0.022	56	66	553.	0.012
17	18	555.	0.050	57	67	552.	0.008
18	19	549.	0.022	58	68	552.	0.005
19	20	551.	0.005	59	69	550.	0.002
20	21	552.	0.005	60	70	592.	0.163
21	23	554.	0.043	61	72	588.	0.145
22	24	549.	0.018	62	73	566.	0.095
23	26	552.	0.004	63	74	565.	0.061
24	28	555.	0.040	64	75	567.	0.070
25	32	555.	0.049	65	76	588.	0.149
26	33	567.	0.120	66	77	585.	0.137
27	34	548.	0.014	67	78	596.	0.153
28	35	551.	0.001	68	79	553.	0.011
29	36	552.	0.006	69	80	555.	0.017
30	37	552.	0.046	70	81	551.	0.002
31	38	563.	0.108	71	82	613.	0.185
32	41	557.	0.045	72	84	599.	0.143
33	42	-	-	73	85	579.	0.115
34	43	551.	0.005	74	86	566.	0.068
35	44	552.	0.000	75	87	561.	0.032
36	45	552.	0.004	76	88	575.	0.100
37	46	554.	0.029	77	89	551.	0.006
38	47	559.	0.086	78	90	553.	0.016
39	48	555.	0.016	79	91	586.	0.164
40	49	563.	0.045	80	92	561.	0.036

$\alpha = 30^{o}$ $\beta = 0^{o}$ $\delta_e = 0^{o}$ $\delta_r = 0^{o}$ TEST NO. 106 RUN NO. 3

MACH	REYN/FT	REL	QS	TWSPH	PT	TT	RSPH(FT)
7.40	9.83E 05	1.04E 06	48.72	581.	239.	1500.	0.006

CHANNEL	T/C	TEMP	QW/QS	CHANNEL	T/C	TEMP	QW/QS
1	1	580.	0.785	41	50	545.	0.002
2	2	-	-	42	51	612.	0.0
3	3	-	-	43	52	543.	0.0
4	4	553.	0.313	44	53	544.	0.0
5	5	535.	0.015	45	54	544.	0.0
6	6	-	-	46	55	544.	0.0
7	7	541.	0.143	47	56	544.	0.004
8	8	534.	0.033	48	57	544.	0.001
9	9	532.	0.008	49	58	545.	0.0
10	10	540.	0.083	50	59	544.	0.0
11	11	534.	0.025	51	60	558.	0.326
12	12	532.	0.013	52	62	549.	0.095
13	13	533.	0.020	53	63	548.	0.058
14	14	534.	0.032	54	64	546.	0.036
15	16	534.	0.005	55	65	546.	0.026
16	17	534.	0.013	56	66	545.	0.007
17	18	539.	0.060	57	67	545.	0.003
18	19	536.	0.021	58	68	544.	0.001
19	20	536.	0.003	59	69	544.	0.0
20	21	536.	0.005	60	70	560.	0.176
21	23	541.	0.052	61	72	560.	0.158
22	24	538.	0.017	62	73	551.	0.100
23	26	538.	0.003	63	74	549.	0.067
24	28	543.	0.048	64	75	547.	0.030
25	32	544.	0.050	65	76	559.	0.157
26	33	549.	0.111	66	77	557.	0.142
27	34	541.	0.011	67	78	562.	0.159
28	35	542.	0.001	68	79	544.	0.008
29	36	542.	0.005	69	80	545.	0.006
30	37	545.	0.046	70	81	544.	0.0
31	38	548.	0.067	71	82	569.	0.185
32	41	546.	0.040	72	84	563.	0.148
33	42	547.	0.045	73	85	554.	0.119
34	43	544.	0.002	74	86	549.	0.067
35	44	544.	0.000	75	87	547.	0.031
36	45	544.	0.003	76	88	554.	0.096
37	46	545.	0.024	77	89	544.	0.006
38	47	546.	0.037	78	90	545.	0.014
39	48	546.	0.017	79	91	553.	0.155
40	49	547.	0.022	80	92	548.	0.030

$\alpha = 30^{\circ}$ $\beta = 0^{\circ}$ $\delta_e = 0^{\circ}$ $\delta_r = 0^{\circ}$ TEST NO. 106 RUN NO. 4

MACH	REYN/FT	REL	QS	TWSPH	PT	TT	RSPH(FT)
7.40	2.00E 06	2.12E 06	69.79	610.	498.	1520.	0.006

CHANNEL	T/C	TEMP	QW/QS	CHANNEL	T/C	TEMP	QW/QS
1	1	606.	0.796	41	50	546.	0.003
2	2	-	-	42	51	612.	0.0
3	3	-	-	43	52	545.	0.0
4	4	569.	0.313	44	53	546.	0.002
5	5	546.	0.015	45	54	545.	0.0
6	6	-	-	46	55	546.	0.0
7	7	554.	0.145	47	56	546.	0.004
8	8	545.	0.034	48	57	546.	0.002
9	9	542.	0.010	49	58	546.	0.0
10	10	552.	0.085	50	59	545.	0.002
11	11	544.	0.025	51	60	568.	0.315
12	12	543.	0.018	52	62	557.	0.093
13	13	544.	0.030	53	63	555.	0.054
14	14	547.	0.042	54	64	552.	0.037
15	16	543.	0.005	55	65	551.	0.027
16	17	544.	0.015	56	66	547.	0.008
17	18	549.	0.062	57	67	546.	0.004
18	19	545.	0.022	58	68	546.	0.002
19	20	542.	0.005	59	69	546.	0.000
20	21	543.	0.005	60	70	571.	0.172
21	23	549.	0.053	61	72	569.	0.160
22	24	545.	0.017	62	73	559.	0.100
23	26	543.	0.003	63	74	554.	0.066
24	28	550.	0.048	64	75	551.	0.029
25	32	549.	0.054	65	76	568.	0.158
26	33	557.	0.111	66	77	568.	0.146
27	34	546.	0.010	67	78	572.	0.162
28	35	544.	0.000	68	79	546.	0.006
29	36	545.	0.004	69	80	547.	0.009
30	37	551.	0.048	70	81	546.	0.002
31	38	555.	0.068	71	82	581.	0.188
32	41	552.	0.043	72	84	577.	0.150
33	42	553.	0.046	73	85	561.	0.120
34	43	545.	0.002	74	86	554.	0.070
35	44	545.	0.000	75	87	550.	0.030
36	45	546.	0.002	76	88	560.	0.098
37	46	551.	0.028	77	89	545.	0.006
38	47	551.	0.046	78	90	547.	0.014
39	48	551.	0.017	79	91	557.	0.148
40	49	551.	0.024	80	92	551.	0.031

$\alpha = 30^{\circ}$ $\beta = 0^{\circ}$ $\delta_e = 0^{\circ}$ $\delta_r = 0^{\circ}$ TEST NO. 106 RUN NO. 5

MACH	REYN/FT	REL	QS	TWSPH	PT	TT	RSPH(FT)
7.40	2.89E 06	3.06E 06	85.16	635.	739.	1545.	0.006

CHANNEL	T/C	TEMP	QW/QS	CHANNEL	T/C	TEMP	QW/QS
1	1	633.	0.772	41	50	550.	0.004
2	2	-	-	42	51	613.	0.001
3	3	-	-	43	52	550.	0.002
4	4	585.	0.319	44	53	549.	0.002
5	5	552.	0.018	45	54	549.	0.001
6	6	-	-	46	55	549.	0.0
7	7	564.	0.148	47	56	550.	0.003
8	8	552.	0.036	48	57	549.	0.001
9	9	549.	0.013	49	58	549.	0.001
10	10	562.	0.084	50	59	549.	0.003
11	11	551.	0.026	51	60	582.	0.298
12	12	551.	0.022	52	62	565.	0.091
13	13	551.	0.040	53	63	562.	0.064
14	14	552.	0.050	54	64	558.	0.040
15	16	550.	0.006	55	65	556.	0.028
16	17	550.	0.014	56	66	551.	0.009
17	18	557.	0.065	57	67	550.	0.006
18	19	551.	0.023	58	68	550.	0.004
19	20	548.	0.004	59	69	549.	0.003
20	21	549.	0.004	60	70	589.	0.171
21	23	556.	0.055	61	72	582.	0.162
22	24	550.	0.017	62	73	566.	0.105
23	26	549.	0.002	63	74	561.	0.068
24	28	557.	0.050	64	75	558.	0.040
25	32	555.	0.058	65	76	582.	0.163
26	33	565.	0.112	66	77	582.	0.148
27	34	550.	0.010	67	78	586.	0.162
28	35	549.	0.001	68	79	551.	0.009
29	36	549.	0.004	69	80	552.	0.012
30	37	557.	0.049	70	81	549.	0.001
31	38	562.	0.071	71	82	599.	0.183
32	41	558.	0.045	72	84	593.	0.148
33	42	560.	0.046	73	85	572.	0.121
34	43	549.	0.003	74	86	561.	0.072
35	44	549.	0.001	75	87	556.	0.029
36	45	550.	0.002	76	88	569.	0.096
37	46	555.	0.029	77	89	549.	0.004
38	47	557.	0.051	78	90	550.	0.014
39	48	556.	0.017	79	91	564.	0.146
40	49	556.	0.026	80	92	556.	0.032

$\alpha = 30^{\circ}$ $\beta = 0^{\circ}$ $\delta_e = 0^{\circ}$ $\delta_r = 0^{\circ}$ TEST NO. 106 RUN NO. 6

MACH	REYN/FT	REL	QS	TWSPH	PT	TT	RSPH(FT)
7.40	3.93E 06	4.17E 06	94.09	649.	981.	1524.	0.006

CHANNEL	T/C	TEMP	QW/QS	CHANNEL	T/C	TEMP	QW/QS
1	1	630.	0.812	41	50	550.	0.004
2	2	-	-	42	51	549.	0.003
3	3	-	-	43	52	548.	0.002
4	4	596.	0.323	44	53	549.	0.002
5	5	550.	0.017	45	54	549.	0.001
6	6	-	-	46	55	549.	0.0
7	7	566.	0.151	47	56	549.	0.004
8	8	549.	0.036	48	57	549.	0.001
9	9	546.	0.013	49	58	655.	0.0
10	10	562.	0.085	50	59	549.	0.002
11	11	547.	0.026	51	60	591.	0.306
12	12	548.	0.023	52	62	567.	0.096
13	13	549.	0.041	53	63	564.	0.063
14	14	550.	0.048	54	64	558.	0.038
15	16	545.	0.006	55	65	555.	0.033
16	17	546.	0.013	56	66	550.	0.007
17	18	556.	0.065	57	67	550.	0.004
18	19	548.	0.023	58	68	550.	0.003
19	20	547.	0.004	59	69	549.	0.002
20	21	547.	0.004	60	70	599.	0.172
21	23	555.	0.055	61	72	591.	0.160
22	24	547.	0.017	62	73	571.	0.105
23	26	547.	0.002	63	74	565.	0.068
24	28	556.	0.051	64	75	561.	0.042
25	32	554.	0.058	65	76	591.	0.163
26	33	567.	0.111	66	77	588.	0.147
27	34	547.	0.011	67	78	597.	0.158
28	35	547.	0.001	68	79	551.	0.008
29	36	548.	0.003	69	80	555.	0.019
30	37	556.	0.052	70	81	550.	0.002
31	38	563.	0.070	71	82	616.	0.167
32	41	559.	0.047	72	84	604.	0.145
33	42	561.	0.046	73	85	579.	0.126
34	43	549.	0.002	74	86	565.	0.072
35	44	549.	0.002	75	87	559.	0.032
36	45	549.	0.001	76	88	575.	0.094
37	46	555.	0.029	77	89	551.	0.006
38	47	558.	0.053	78	90	554.	0.015
39	48	556.	0.018	79	91	570.	0.140
40	49	559.	0.026	80	92	559.	0.031

$\alpha = 30^{o}$ $\beta = 0^{o}$ $\delta_e = 0^{o}$ $\delta_r = 0^{o}$ TEST NO. 106 RUN NO. 58

MACH	REYN/FT	REL	QS	TWSPH	PT	TT	RSPH(FT)
7.40	6.83E 06	7.24E 06	99.82	650.	1494.	1409.	0.006

CHANNEL	T/C	TEMP	QW/QS	CHANNEL	T/C	TEMP	QW/QS
1	1	644.	0.777	41	50	546.	0.004
2	2	-	-	42	51	546.	0.003
3	3	-	-	43	52	545.	0.002
4	4	590.	0.336	44	53	546.	0.002
5	5	550.	0.016	45	54	545.	0.001
6	6	-	-	46	55	545.	0.0
7	7	565.	0.158	47	56	-	-
8	8	549.	0.036	48	57	546.	0.001
9	9	-	-	49	58	546.	0.002
10	10	562.	0.090	50	59	545.	0.003
11	11	548.	0.026	51	60	583.	0.323
12	12	549.	0.026	52	62	564.	0.106
13	13	550.	0.046	53	63	560.	0.069
14	14	550.	0.048	54	64	552.	0.041
15	16	546.	0.007	55	65	557.	0.040
16	17	546.	0.012	56	66	547.	0.007
17	18	556.	0.066	57	67	546.	0.003
18	19	547.	0.023	58	68	546.	0.001
19	20	547.	0.006	59	69	546.	0.002
20	21	548.	0.006	60	70	589.	0.174
21	23	554.	0.057	61	72	588.	0.165
22	24	543.	0.001	62	73	566.	0.117
23	26	547.	0.003	63	74	562.	0.080
24	28	554.	0.052	64	75	560.	0.045
25	32	555.	0.090	65	76	587.	0.169
26	33	564.	0.125	66	77	584.	0.151
27	34	544.	0.011	67	78	593.	0.166
28	35	545.	0.000	68	79	546.	0.004
29	36	546.	0.004	69	80	546.	0.004
30	37	571.	0.226	70	81	546.	0.001
31	38	560.	0.079	71	82	609.	0.185
32	41	577.	0.240	72	84	601.	0.153
33	42	557.	0.054	73	85	576.	0.129
34	43	545.	0.003	74	86	563.	0.078
35	44	545.	0.001	75	87	556.	0.031
36	45	546.	0.002	76	88	569.	0.095
37	46	563.	0.140	77	89	546.	0.005
38	47	557.	0.076	78	90	548.	0.014
39	48	565.	0.092	79	91	578.	0.134
40	49	564.	0.092	80	92	556.	0.032

$\alpha = 30^{\circ}$ $\beta = 0^{\circ}$ $\delta_e = +10^{\circ}$ $\delta_r = \pm 13^{\circ}$ TEST NO. 106 RUN NO. 14

MACH	REYN/FT	REL	QS	TWSPH	PT	TT	RSPH(FT)
7.40	9.42E 05	1.00E 06	51.99	602.	246.	1564.	0.006

CHANNEL	T/C	TEMP	QW/QS	CHANNEL	T/C	TEMP	QW/QS
1	1	601.	0.800	41	50	550.	0.002
2	2	-	-	42	51	551.	0.006
3	3	-	-	43	52	550.	0.0
4	4	587.	0.316	44	53	550.	0.0
5	5	552.	0.019	45	54	550.	0.0
6	6	-	-	46	55	549.	0.0
7	7	559.	0.144	47	56	551.	0.006
8	8	551.	0.036	48	57	550.	0.002
9	9	550.	0.008	49	58	549.	0.0
10	10	557.	0.083	50	59	548.	0.0
11	11	551.	0.025	51	60	569.	0.318
12	12	551.	0.014	52	62	558.	0.095
13	13	552.	0.021	53	63	555.	0.060
14	14	553.	0.035	54	64	553.	0.039
15	16	551.	0.004	55	65	556.	0.060
16	17	551.	0.013	56	66	551.	0.010
17	18	555.	0.060	57	67	550.	0.006
18	19	552.	0.022	58	68	550.	0.003
19	20	551.	0.0	59	69	548.	0.001
20	21	551.	0.005	60	70	572.	0.177
21	23	555.	0.053	61	72	568.	0.163
22	24	551.	0.018	62	73	558.	0.104
23	26	551.	0.002	63	74	555.	0.069
24	28	554.	0.047	64	75	555.	0.055
25	32	554.	0.050	65	76	567.	0.164
26	33	560.	0.116	66	77	567.	0.147
27	34	551.	0.012	67	78	570.	0.166
28	35	550.	0.001	68	79	549.	0.006
29	36	551.	0.005	69	80	548.	0.003
30	37	554.	0.047	70	81	548.	0.002
31	38	556.	0.072	71	82	578.	0.187
32	41	554.	0.043	72	84	573.	0.152
33	42	555.	0.046	73	85	560.	0.126
34	43	550.	0.003	74	86	555.	0.070
35	44	550.	0.001	75	87	554.	0.054
36	45	551.	0.004	76	88	560.	0.100
37	46	553.	0.026	77	89	547.	0.006
38	47	554.	0.049	78	90	546.	0.006
39	48	553.	0.017	79	91	569.	0.183
40	49	553.	0.016	80	92	556.	0.070

$\alpha = 30^{\circ}$ $\beta = 0^{\circ}$ $\delta_e = +10^{\circ}$ $\delta_r = \pm 13^{\circ}$ TEST NO. 106 RUN NO. 15

MACH	REYN/FT	REL	QS	TWSPH	PT	TT	RSPH(FT)
7.40	2.37E 06	2.52E 06	81.54	622.	624.	1569.	0.006

CHANNEL	T/C	TEMP	QW/QS	CHANNEL	T/C	TEMP	QW/QS
1	1	612.	0.828	41	50	551.	0.003
2	2	-	-	42	51	551.	0.004
3	3	-	-	43	52	551.	0.0
4	4	599.	0.315	44	53	551.	0.0
5	5	551.	0.018	45	54	551.	0.0
6	6	-	-	46	55	549.	0.0
7	7	560.	0.144	47	56	551.	0.004
8	8	551.	0.035	48	57	551.	0.001
9	9	548.	0.012	49	58	550.	0.0
10	10	559.	0.081	50	59	550.	0.0
11	11	550.	0.024	51	60	594.	0.299
12	12	550.	0.021	52	62	562.	0.094
13	13	553.	0.034	53	63	559.	0.067
14	14	554.	0.042	54	64	556.	0.047
15	16	550.	0.006	55	65	561.	0.067
16	17	550.	0.014	56	66	552.	0.008
17	18	556.	0.060	57	67	551.	0.005
18	19	551.	0.022	58	68	551.	0.003
19	20	549.	0.004	59	69	550.	0.002
20	21	550.	0.004	60	70	578.	0.174
21	23	555.	0.050	61	72	576.	0.158
22	24	550.	0.019	62	73	562.	0.103
23	26	551.	0.002	63	74	559.	0.068
24	28	556.	0.045	64	75	561.	0.064
25	32	554.	0.052	65	76	575.	0.160
26	33	563.	0.113	66	77	575.	0.146
27	34	551.	0.010	67	78	579.	0.162
28	35	550.	0.001	68	79	552.	0.009
29	36	551.	0.004	69	80	553.	0.013
30	37	556.	0.044	70	81	550.	0.001
31	38	560.	0.070	71	82	587.	0.189
32	41	557.	0.045	72	84	584.	0.148
33	42	558.	0.046	73	85	567.	0.118
34	43	551.	0.003	74	86	559.	0.072
35	44	551.	0.001	75	87	559.	0.051
36	45	551.	0.002	76	88	565.	0.095
37	46	555.	0.030	77	89	549.	0.004
38	47	560.	0.084	78	90	548.	0.004
39	48	555.	0.019	79	91	577.	0.174
40	49	556.	0.017	80	92	561.	0.068

$\alpha = 30^{\circ}$ $\beta = 0^{\circ}$ $\delta_e = +10^{\circ}$ $\delta_r = \pm 13^{\circ}$ TEST NO. 106 RUN NO. 16

MACH	REYN/FT	REL	QS	TWSPH	PT	TT	RSPH(FT)
7.40	3.96E 06	4.20E 06	93.82	648.	984.	1519.	0.006

CHANNEL	T/C	TEMP	QW/QS	CHANNEL	T/C	TEMP	QW/QS
1	1	648.	0.755	41	50	553.	0.004
2	2	-	-	42	51	553.	0.003
3	3	-	-	43	52	552.	0.0
4	4	622.	0.315	44	53	552.	0.0
5	5	553.	0.017	45	54	552.	0.0
6	6	-	-	46	55	551.	0.0
7	7	568.	0.153	47	56	553.	0.004
8	8	553.	0.037	48	57	552.	0.001
9	9	550.	0.013	49	58	552.	0.0
10	10	565.	0.086	50	59	551.	0.0
11	11	552.	0.027	51	60	591.	0.322
12	12	553.	0.024	52	62	569.	0.100
13	13	557.	0.041	53	63	565.	0.066
14	14	558.	0.044	54	64	560.	0.043
15	16	551.	0.007	55	65	587.	0.179
16	17	552.	0.013	56	66	553.	0.007
17	18	560.	0.064	57	67	552.	0.004
18	19	553.	0.022	58	68	552.	0.002
19	20	552.	0.004	59	69	550.	0.001
20	21	552.	0.004	60	70	596.	0.170
21	23	559.	0.054	61	72	590.	0.161
22	24	551.	0.020	62	73	571.	0.107
23	26	552.	0.002	63	74	566.	0.072
24	28	559.	0.048	64	75	572.	0.095
25	32	557.	0.054	65	76	589.	0.166
26	33	570.	0.114	66	77	587.	0.154
27	34	552.	0.008	67	78	594.	0.160
28	35	551.	0.000	68	79	553.	0.013
29	36	552.	0.003	69	80	557.	0.026
30	37	560.	0.048	70	81	551.	0.006
31	38	565.	0.069	71	82	611.	0.177
32	41	561.	0.044	72	84	601.	0.150
33	42	567.	0.091	73	85	577.	0.128
34	43	552.	0.002	74	86	566.	0.074
35	44	552.	0.002	75	87	571.	0.099
36	45	552.	0.001	76	88	573.	0.091
37	46	558.	0.030	77	89	550.	0.007
38	47	570.	0.123	78	90	549.	0.006
39	48	560.	0.020	79	91	590.	0.169
40	49	563.	0.036	80	92	567.	0.067

$\alpha = 30^{\circ}$ $\beta = -5^{\circ}$ $\delta_e = +10^{\circ}$ $\delta_r = \pm 13^{\circ}$ TEST NO. 106 RUN NO. 23

MACH	REYN/FT	REL	QS	TWSPH	PT	TT	RSPH(FT)
7.40	9.98E 05	1.06E 06	49.22	593.	245.	1509.	0.006

CHANNEL	T/C	TEMP	QW/QS	CHANNEL	T/C	TEMP	QW/QS
1	1	584.	0.891	41	50	549.	0.002
2	2	-	-	42	51	549.	0.004
3	3	-	-	43	52	549.	0.0
4	4	578.	0.314	44	53	549.	0.0
5	5	551.	0.017	45	54	549.	0.0
6	6	-	-	46	55	550.	0.0
7	7	556.	0.144	47	56	549.	0.003
8	8	551.	0.049	48	57	549.	0.0
9	9	549.	0.010	49	58	549.	0.0
10	10	555.	0.084	50	59	549.	0.0
11	11	551.	0.037	51	60	568.	0.394
12	12	549.	0.008	52	62	556.	0.108
13	13	549.	0.012	53	63	554.	0.067
14	14	549.	0.016	54	64	552.	0.046
15	16	549.	0.003	55	65	556.	0.071
16	17	549.	0.005	56	66	550.	0.008
17	18	553.	0.063	57	67	550.	0.004
18	19	551.	0.033	58	68	550.	0.002
19	20	549.	0.004	59	69	550.	0.001
20	21	550.	0.004	60	70	563.	0.195
21	23	552.	0.055	61	72	568.	0.165
22	24	550.	0.027	62	73	557.	0.103
23	26	550.	0.002	63	74	555.	0.073
24	28	552.	0.049	64	75	558.	0.060
25	32	551.	0.053	65	76	568.	0.176
26	33	559.	0.152	66	77	567.	0.167
27	34	549.	0.020	67	78	573.	0.190
28	35	549.	0.001	68	79	550.	0.0
29	36	549.	0.006	69	80	550.	0.0
30	37	551.	0.048	70	81	550.	0.0
31	38	555.	0.084	71	82	574.	0.243
32	41	551.	0.044	72	84	576.	0.173
33	42	553.	0.053	73	85	563.	0.130
34	43	550.	0.007	74	86	557.	0.075
35	44	549.	0.001	75	87	556.	0.050
36	45	549.	0.003	76	88	565.	0.108
37	46	550.	0.028	77	89	551.	0.009
38	47	551.	0.041	78	90	551.	0.006
39	48	550.	0.017	79	91	582.	0.215
40	49	552.	0.023	80	92	566.	0.104

$\alpha = 30^{\circ}$ $\beta = -5^{\circ}$ $\delta_e = +10^{\circ}$ $\delta_r = \pm 13^{\circ}$ TEST NO. 106 RUN NO. 24

MACH	REYN/FT	REL	QS	TWSPH	PT	TT	RSPH(FT)
7.40	4.12E 06	4.37E 06	87.14	646.	965.	1466.	0.006

CHANNEL	T/C	TEMP	QW/QS	CHANNEL	T/C	TEMP	QW/QS
1	1	642.	0.910	41	50	554.	0.002
2	2	-	-	42	51	555.	0.002
3	3	-	-	43	52	554.	0.0
4	4	620.	0.328	44	53	554.	0.0
5	5	559.	0.017	45	54	554.	0.0
6	6	-	-	46	55	554.	0.0
7	7	572.	0.158	47	56	555.	0.002
8	8	560.	0.052	48	57	554.	0.0
9	9	556.	0.017	49	58	554.	0.0
10	10	570.	0.090	50	59	554.	0.0
11	11	560.	0.038	51	60	576.	0.405
12	12	555.	0.013	52	62	575.	0.115
13	13	557.	0.020	53	63	569.	0.073
14	14	557.	0.020	54	64	563.	0.049
15	16	555.	0.004	55	65	578.	0.105
16	17	555.	0.006	56	66	555.	0.007
17	18	565.	0.068	57	67	555.	0.004
18	19	560.	0.034	58	68	554.	0.002
19	20	555.	0.003	59	69	554.	0.002
20	21	556.	0.008	60	70	581.	0.201
21	23	564.	0.058	61	72	598.	0.172
22	24	558.	0.028	62	73	576.	0.110
23	26	555.	0.004	63	74	569.	0.073
24	28	564.	0.052	64	75	573.	0.067
25	32	562.	0.056	65	76	584.	0.188
26	33	580.	0.153	66	77	584.	0.173
27	34	557.	0.020	67	78	591.	0.191
28	35	554.	0.001	68	79	556.	0.004
29	36	555.	0.004	69	80	556.	0.008
30	37	563.	0.052	70	81	554.	0.001
31	38	571.	0.087	71	82	601.	0.243
32	41	562.	0.048	72	84	618.	0.173
33	42	566.	0.056	73	85	589.	0.144
34	43	556.	0.014	74	86	572.	0.087
35	44	554.	0.001	75	87	570.	0.057
36	45	554.	0.002	76	88	585.	0.106
37	46	559.	0.034	77	89	555.	0.004
38	47	562.	0.089	78	90	555.	0.003
39	48	559.	0.019	79	91	614.	0.204
40	49	560.	0.024	80	92	583.	0.100

$\alpha = 53^{\circ}$ $\beta = 0^{\circ}$ $\delta_e = 0^{\circ}$ $\delta_r = 0^{\circ}$ TEST NO. 106 RUN NO. 7

MACH	REYN/FT	REL	QS	TWSPH	PT	TT	RSPH(FT)
7.40	1.14E 06	1.21E 06	44.18	621.	257.	1431.	0.006

CHANNEL	T/C	TEMP	QW/QS	CHANNEL	T/C	TEMP	QW/QS
1	1	583.	0.686	41	50	553.	0.0
2	2	-	-	42	51	553.	0.0
3	3	-	-	43	52	553.	0.0
4	4	575.	0.465	44	53	553.	0.0
5	5	555.	0.009	45	54	553.	0.001
6	6	-	-	46	55	553.	0.0
7	7	569.	0.248	47	56	553.	0.001
8	8	555.	0.038	48	57	553.	0.001
9	9	553.	0.008	49	58	646.	0.001
10	10	568.	0.157	50	59	553.	0.002
11	11	555.	0.027	51	60	572.	0.181
12	12	554.	0.011	52	62	563.	0.134
13	13	554.	0.014	53	63	561.	0.094
14	14	554.	0.015	54	64	558.	0.066
15	16	554.	0.005	55	65	556.	0.049
16	17	554.	0.008	56	66	553.	0.0
17	18	563.	0.121	57	67	553.	0.0
18	19	555.	0.022	58	68	553.	0.0
19	20	554.	0.003	59	69	553.	0.002
20	21	554.	0.005	60	70	577.	0.110
21	23	561.	0.102	61	72	571.	0.171
22	24	554.	0.020	62	73	564.	0.134
23	26	554.	0.005	63	74	561.	0.101
24	28	561.	0.091	64	75	559.	0.065
25	32	559.	0.095	65	76	571.	0.185
26	33	562.	0.123	66	77	571.	0.168
27	34	554.	0.009	67	78	573.	0.181
28	35	553.	0.001	68	79	552.	0.002
29	36	554.	0.009	69	80	553.	0.002
30	37	560.	0.084	70	81	552.	0.004
31	38	562.	0.111	71	82	583.	0.132
32	41	560.	0.080	72	84	575.	0.157
33	42	560.	0.086	73	85	566.	0.157
34	43	553.	0.000	74	86	561.	0.111
35	44	553.	0.001	75	87	559.	0.080
36	45	553.	0.001	76	88	557.	0.031
37	46	557.	0.055	77	89	553.	0.001
38	47	560.	0.103	78	90	552.	0.001
39	48	560.	0.053	79	91	557.	0.049
40	49	559.	0.065	80	92	558.	0.047

$\alpha = 53^{\circ}$ $\beta = 0^{\circ}$ $\delta_e = 0^{\circ}$ $\delta_r = 0^{\circ}$ TEST NO. 106 RUN NO. 8

MACH	REYN/FT	REL	QS	TWSPH	PT	TT	RSPH(FT)
7.40	1.73E 06	1.83E 06	76.78	655.	494.	1650.	0.006

CHANNEL	T/C	TEMP	QW/QS	CHANNEL	T/C	TEMP	QW/QS
1	1	591.	0.696	41	50	550.	0.001
2	2	-	-	42	51	548.	0.001
3	3	-	-	43	52	548.	0.0
4	4	578.	0.462	44	53	549.	0.002
5	5	545.	0.014	45	54	550.	0.002
6	6	-	-	46	55	550.	0.0
7	7	567.	0.244	47	56	549.	0.001
8	8	544.	0.039	48	57	550.	0.002
9	9	540.	0.011	49	58	550.	0.002
10	10	564.	0.154	50	59	550.	0.000
11	11	542.	0.027	51	60	578.	0.186
12	12	539.	0.009	52	62	565.	0.126
13	13	540.	0.012	53	63	562.	0.092
14	14	540.	0.014	54	64	558.	0.071
15	16	539.	0.003	55	65	554.	0.050
16	17	539.	0.006	56	66	550.	0.0
17	18	556.	0.120	57	67	550.	0.0
18	19	543.	0.023	58	68	550.	0.0
19	20	540.	0.003	59	69	550.	0.002
20	21	541.	0.003	60	70	583.	0.108
21	23	555.	0.101	61	72	579.	0.165
22	24	543.	0.020	62	73	566.	0.130
23	26	542.	0.004	63	74	563.	0.106
24	28	556.	0.088	64	75	562.	0.081
25	32	556.	0.097	65	76	579.	0.178
26	33	561.	0.121	66	77	578.	0.166
27	34	546.	0.010	67	78	583.	0.174
28	35	546.	0.001	68	79	550.	0.002
29	36	547.	0.006	69	80	551.	0.002
30	37	559.	0.083	70	81	551.	0.002
31	38	563.	0.111	71	82	601.	0.127
32	41	560.	0.079	72	84	586.	0.150
33	42	561.	0.086	73	85	571.	0.150
34	43	549.	0.0	74	86	564.	0.109
35	44	549.	0.001	75	87	561.	0.077
36	45	549.	0.001	76	88	558.	0.033
37	46	557.	0.057	77	89	551.	0.0
38	47	561.	0.114	78	90	551.	0.001
39	48	561.	0.054	79	91	558.	0.047
40	49	562.	0.067	80	92	559.	0.046

$\alpha = 53^{\circ}$ $\beta = 0^{\circ}$ $\delta_e = 0^{\circ}$ $\delta_r = 0^{\circ}$ TEST NO. 106 RUN NO. 9

MACH	REYN/FT	REL	QS	TWSPH	PT	TT	RSPH(FT)
7.40	2.99E 06	3.17E 06	79.26	665.	739.	1514.	0.006

CHANNEL	T/C	TEMP	QW/QS	CHANNEL	T/C	TEMP	QW/QS
1	1	595.	0.693	41	50	552.	0.001
2	2	-	-	42	51	551.	0.000
3	3	-	-	43	52	551.	0.0
4	4	584.	0.469	44	53	551.	0.001
5	5	550.	0.018	45	54	552.	0.001
6	6	-	-	46	55	551.	0.0
7	7	573.	0.251	47	56	552.	0.000
8	8	549.	0.039	48	57	552.	0.002
9	9	546.	0.014	49	58	552.	0.002
10	10	571.	0.158	50	59	552.	0.001
11	11	547.	0.027	51	60	582.	0.189
12	12	545.	0.008	52	62	570.	0.129
13	13	546.	0.010	53	63	567.	0.094
14	14	546.	0.011	54	64	562.	0.075
15	16	546.	0.003	55	65	557.	0.108
16	17	546.	0.004	56	66	551.	0.0
17	18	563.	0.125	57	67	552.	0.0
18	19	548.	0.024	58	68	552.	0.0
19	20	547.	0.003	59	69	552.	0.002
20	21	548.	0.002	60	70	585.	0.105
21	23	561.	0.105	61	72	584.	0.170
22	24	547.	0.020	62	73	570.	0.131
23	26	549.	0.004	63	74	567.	0.107
24	28	562.	0.093	64	75	570.	0.118
25	32	560.	0.102	65	76	584.	0.178
26	33	565.	0.123	66	77	582.	0.164
27	34	549.	0.010	67	78	588.	0.175
28	35	550.	0.002	68	79	553.	0.002
29	36	550.	0.004	69	80	553.	0.002
30	37	563.	0.086	70	81	553.	0.003
31	38	569.	0.114	71	82	606.	0.127
32	41	565.	0.084	72	84	590.	0.149
33	42	566.	0.089	73	85	576.	0.148
34	43	552.	0.001	74	86	568.	0.113
35	44	552.	0.002	75	87	564.	0.077
36	45	552.	0.002	76	88	560.	0.033
37	46	564.	0.066	77	89	551.	0.002
38	47	566.	0.116	78	90	552.	0.002
39	48	583.	0.110	79	91	559.	0.049
40	49	573.	0.091	80	92	561.	0.048

$\alpha = 53^{\circ}$ $\beta = 0^{\circ}$ $\delta_e = 0^{\circ}$ $\delta_r = 0^{\circ}$ TEST NO. 106 RUN NO. 10

MACH	REYN/FT	REL	QS	TWSPH	PT	TT	RSPH(FT)
7.40	4.05E 06	4.29E 06	85.06	687.	968.	1485.	0.006

CHANNEL	T/C	TEMP	QW/QS	CHANNEL	T/C	TEMP	QW/QS
1	1	611.	0.687	41	50	554.	0.001
2	2	-	-	42	51	555.	0.001
3	3	-	-	43	52	554.	0.0
4	4	599.	0.485	44	53	557.	0.009
5	5	559.	0.018	45	54	555.	0.003
6	6	-	-	46	55	555.	0.0
7	7	585.	0.261	47	56	556.	0.002
8	8	558.	0.040	48	57	559.	0.013
9	9	555.	0.014	49	58	557.	0.008
10	10	583.	0.165	50	59	554.	0.002
11	11	555.	0.031	51	60	593.	0.186
12	12	554.	0.008	52	62	579.	0.139
13	13	555.	0.012	53	63	575.	0.101
14	14	555.	0.012	54	64	570.	0.089
15	16	555.	0.004	55	65	579.	0.170
16	17	554.	0.004	56	66	556.	0.001
17	18	574.	0.130	57	67	556.	0.002
18	19	556.	0.025	58	68	556.	0.002
19	20	554.	0.004	59	69	554.	0.001
20	21	554.	0.003	60	70	598.	0.108
21	23	570.	0.109	61	72	595.	0.174
22	24	554.	0.019	62	73	580.	0.141
23	26	555.	0.003	63	74	575.	0.113
24	28	571.	0.101	64	75	583.	0.177
25	32	569.	0.110	65	76	595.	0.189
26	33	574.	0.126	66	77	594.	0.176
27	34	555.	0.010	67	78	599.	0.180
28	35	554.	0.002	68	79	554.	0.001
29	36	555.	0.003	69	80	555.	0.005
30	37	572.	0.093	70	81	555.	0.005
31	38	578.	0.118	71	82	618.	0.129
32	41	572.	0.092	72	84	605.	0.156
33	42	574.	0.097	73	85	586.	0.169
34	43	555.	0.C	74	86	588.	0.247
35	44	555.	0.001	75	87	570.	0.090
36	45	555.	0.002	76	88	565.	0.036
37	46	568.	0.068	77	89	554.	0.002
38	47	573.	0.142	78	90	554.	0.004
39	48	580.	0.082	79	91	563.	0.047
40	49	574.	0.080	80	92	565.	0.051

$\alpha = 53^{\circ}$ $\beta = 0^{\circ}$ $\delta_e = -7.5^{\circ}$ $\delta_r = 0^{\circ}$ TEST NO. 106 RUN NO. 11

MACH	REYN/FT	REL	QS	TWSPH	PT	TT	RSPH(FT)
7.40	1.04E 06	1.10E 06	46.89	605.	247.	1477.	0.006

CHANNEL	T/C	TEMP	QW/QS	CHANNEL	T/C	TEMP	QW/QS
1	1	562.	0.695	41	50	559.	0.0
2	2	-	-	42	51	617.	0.0
3	3	-	-	43	52	557.	0.0
4	4	555.	0.472	44	53	557.	0.0
5	5	531.	0.015	45	54	557.	0.001
6	6	-	-	46	55	557.	0.0
7	7	550.	0.248	47	56	557.	0.0
8	8	533.	0.041	48	57	557.	0.001
9	9	530.	0.010	49	58	557.	0.002
10	10	550.	0.154	50	59	557.	0.002
11	11	535.	0.029	51	60	574.	0.190
12	12	530.	0.012	52	62	566.	0.126
13	13	531.	0.014	53	63	564.	0.093
14	14	532.	0.017	54	64	562.	0.063
15	16	532.	0.004	55	65	561.	0.041
16	17	531.	0.007	56	66	556.	0.0
17	18	550.	0.122	57	67	556.	0.0
18	19	541.	0.024	58	68	557.	0.0
19	20	534.	0.0	59	69	556.	0.0
20	21	534.	0.004	60	70	577.	0.110
21	23	555.	0.101	61	72	574.	0.176
22	24	546.	0.020	62	73	566.	0.132
23	26	541.	0.005	63	74	564.	0.100
24	28	560.	0.087	64	75	561.	0.041
25	32	561.	0.096	65	76	574.	0.183
26	33	564.	0.123	66	77	575.	0.175
27	34	555.	0.008	67	78	576.	0.180
28	35	552.	0.002	68	79	556.	0.001
29	36	551.	0.008	69	80	557.	0.001
30	37	564.	0.081	70	81	556.	0.002
31	38	565.	0.115	71	82	588.	0.132
32	41	565.	0.079	72	84	579.	0.151
33	42	565.	0.085	73	85	569.	0.149
34	43	558.	0.000	74	86	564.	0.108
35	44	556.	0.001	75	87	561.	0.049
36	45	556.	0.001	76	88	561.	0.026
37	46	562.	0.058	77	89	556.	0.001
38	47	562.	0.055	78	90	555.	0.003
39	48	564.	0.051	79	91	559.	0.050
40	49	564.	0.063	80	92	560.	0.048

$\alpha = 53^{\circ}$ $\beta = 0^{\circ}$ $\delta_e = -7.5^{\circ}$ $\delta_r = 0^{\circ}$ TEST NO. 106 RUN NO. 12

MACH	REYN/FT	REL	QS	TWSPH	PT	TT	RSPH(FT)
7.40	2.35E 06	2.49E 06	76.21	660.	609.	1556.	0.006

CHANNEL	T/C	TEMP	QW/QS	CHANNEL	T/C	TEMP	QW/QS
1	1	597.	0.657	41	50	543.	0.001
2	2	-	-	42	51	543.	0.001
3	3	-	-	43	52	543.	0.0
4	4	584.	0.461	44	53	543.	0.002
5	5	546.	0.015	45	54	543.	0.001
6	6	-	-	46	55	543.	0.0
7	7	570.	0.247	47	56	544.	0.001
8	8	545.	0.039	48	57	544.	0.003
9	9	542.	0.012	49	58	544.	0.002
10	10	568.	0.154	50	59	543.	0.001
11	11	544.	0.027	51	60	577.	0.188
12	12	542.	0.008	52	62	563.	0.128
13	13	543.	0.011	53	63	562.	0.212
14	14	543.	0.012	54	64	556.	0.192
15	16	543.	0.004	55	65	553.	0.096
16	17	542.	0.005	56	66	544.	0.003
17	18	560.	0.122	57	67	544.	0.002
18	19	545.	0.024	58	68	544.	0.002
19	20	542.	0.005	59	69	543.	0.001
20	21	543.	0.003	60	70	581.	0.103
21	23	557.	0.103	61	72	577.	0.167
22	24	543.	0.020	62	73	564.	0.132
23	26	544.	0.005	63	74	558.	0.102
24	28	557.	0.090	64	75	554.	0.115
25	32	555.	0.102	65	76	576.	0.177
26	33	560.	0.122	66	77	576.	0.161
27	34	544.	0.009	67	78	580.	0.175
28	35	543.	0.002	68	79	543.	0.002
29	36	543.	0.003	69	80	543.	0.004
30	37	556.	0.083	70	81	543.	0.003
31	38	562.	0.110	71	82	598.	0.125
32	41	557.	0.080	72	84	584.	0.150
33	42	559.	0.120	73	85	567.	0.148
34	43	543.	0.000	74	86	559.	0.112
35	44	543.	0.001	75	87	552.	0.049
36	45	544.	0.002	76	88	550.	0.030
37	46	553.	0.063	77	89	541.	0.002
38	47	552.	0.075	78	90	542.	0.007
39	48	557.	0.057	79	91	554.	0.049
40	49	556.	0.068	80	92	551.	0.049

$\alpha = 53^{\circ}$ $\beta = 0^{\circ}$ $\delta_e = -7.5^{\circ}$ $\delta_r = 0^{\circ}$ TEST NO. 106 RUN NO. 13

MACH	REYN/FT	REL	QS	TWSPH	PT	TT	RSPH(FT)
7.40	3.76E 06	3.98E 06	93.29	671.	961.	1545.	0.006

CHANNEL	T/C	TEMP	QW/QS	CHANNEL	T/C	TEMP	QW/QS
1	1	588.	0.712	41	50	544.	0.001
2	2	-	-	42	51	543.	0.001
3	3	-	-	43	52	544.	0.0
4	4	575.	0.475	44	53	544.	0.002
5	5	539.	0.018	45	54	544.	0.002
6	6	-	-	46	55	544.	0.001
7	7	565.	0.254	47	56	544.	0.001
8	8	538.	0.038	48	57	544.	0.003
9	9	534.	0.014	49	58	544.	0.002
10	10	564.	0.159	50	59	544.	0.001
11	11	536.	0.029	51	60	580.	0.186
12	12	535.	0.008	52	62	566.	0.136
13	13	536.	0.012	53	63	579.	0.266
14	14	537.	0.012	54	64	569.	0.226
15	16	537.	0.004	55	65	568.	0.161
16	17	536.	0.004	56	66	544.	0.003
17	18	556.	0.126	57	67	544.	0.003
18	19	539.	0.024	58	68	545.	0.003
19	20	537.	0.002	59	69	544.	0.003
20	21	538.	0.002	60	70	585.	0.106
21	23	555.	0.104	61	72	582.	0.171
22	24	539.	0.020	62	73	567.	0.133
23	26	539.	0.004	63	74	571.	0.227
24	28	556.	0.095	64	75	567.	0.149
25	32	556.	0.112	65	76	582.	0.179
26	33	561.	0.128	66	77	581.	0.171
27	34	542.	0.010	67	78	586.	0.176
28	35	542.	0.002	68	79	546.	0.003
29	36	542.	0.003	69	80	547.	0.010
30	37	561.	0.107	70	81	545.	0.004
31	38	566.	0.165	71	82	607.	0.128
32	41	564.	0.075	72	84	591.	0.152
33	42	575.	0.170	73	85	574.	0.153
34	43	543.	0.000	74	86	566.	0.155
35	44	544.	0.002	75	87	563.	0.125
36	45	544.	0.002	76	88	554.	0.032
37	46	560.	0.060	77	89	544.	0.003
38	47	556.	0.110	78	90	546.	0.008
39	48	571.	0.060	79	91	553.	0.050
40	49	565.	0.112	80	92	555.	0.051

$\alpha = 53^\circ$ $\beta = -5^\circ$ $\delta_e = -7.5^\circ$ $\delta_r = 0^\circ$ TEST NO. 106 RUN NO. 25

MACH	REYN/FT	REL	QS	TWSPH	PT	TT	RSPH(FT)
7.40	1.04E 06	1.10E 06	47.66	603.	249.	1486.	0.006

CHANNEL	T/C	TEMP	QW/QS	CHANNEL	T/C	TEMP	QW/QS
1	1	556.	0.709	41	50	542.	0.002
2	2	-	-	42	51	542.	0.001
3	3	-	-	43	52	542.	0.0
4	4	562.	0.456	44	53	542.	0.0
5	5	546.	0.006	45	54	542.	0.001
6	6	-	-	46	55	542.	0.0
7	7	553.	0.247	47	56	542.	0.001
8	8	542.	0.051	48	57	542.	0.001
9	9	540.	0.009	49	58	542.	0.001
10	10	553.	0.159	50	59	542.	0.001
11	11	542.	0.038	51	60	556.	0.245
12	12	540.	0.008	52	62	553.	0.147
13	13	541.	0.012	53	63	550.	0.103
14	14	541.	0.011	54	64	547.	0.072
15	16	541.	0.002	55	65	546.	0.042
16	17	541.	0.005	56	66	542.	0.001
17	18	550.	0.122	57	67	542.	0.001
18	19	543.	0.033	58	68	542.	0.001
19	20	542.	0.003	59	69	542.	0.001
20	21	542.	0.003	60	70	559.	0.136
21	23	549.	0.101	61	72	564.	0.189
22	24	542.	0.026	62	73	554.	0.142
23	26	542.	0.003	63	74	551.	0.104
24	28	549.	0.089	64	75	547.	0.051
25	32	548.	0.098	65	76	564.	0.201
26	33	553.	0.150	66	77	555.	0.188
27	34	542.	0.014	67	78	558.	0.204
28	35	542.	0.001	68	79	541.	0.004
29	36	542.	0.007	69	80	542.	0.0
30	37	548.	0.085	70	81	542.	0.002
31	38	552.	0.126	71	82	570.	0.160
32	41	548.	0.079	72	84	560.	0.178
33	42	550.	0.091	73	85	559.	0.170
34	43	-	-	74	86	553.	0.118
35	44	542.	0.002	75	87	548.	0.060
36	45	542.	0.001	76	88	550.	0.043
37	46	546.	0.060	77	89	542.	0.002
38	47	544.	0.040	78	90	542.	0.005
39	48	548.	0.063	79	91	550.	0.056
40	49	549.	0.068	80	92	548.	0.047

$\alpha = 53^\circ$ $\beta = -5^\circ$ $\delta_e = -7.5^\circ$ $\delta_r = 0^\circ$ TEST NO. 106 RUN NO. 26

MACH	KEYN/FT	REL	QS	TWSPH	PT	TT	RSPH(FT)
7.40	3.97E 06	4.22E 06	88.75	669.	967.	1501.	0.006

CHANNEL	T/C	TEMP	QW/QS	CHANNEL	T/C	TEMP	QW/QS
1	1	583.	0.731	41	50	547.	0.002
2	2	-	-	42	51	614.	0.0
3	3	-	-	43	52	546.	0.0
4	4	595.	0.476	44	53	547.	0.002
5	5	547.	0.017	45	54	546.	0.002
6	6	-	-	46	55	546.	0.0
7	7	572.	0.260	47	56	547.	0.001
8	8	547.	0.053	48	57	547.	0.002
9	9	543.	0.016	49	58	546.	0.001
10	10	572.	0.166	50	59	546.	0.001
11	11	547.	0.039	51	60	578.	0.251
12	12	543.	0.007	52	62	573.	0.150
13	13	544.	0.011	53	63	567.	0.109
14	14	544.	0.011	54	64	560.	0.079
15	16	544.	0.003	55	65	559.	0.075
16	17	543.	0.004	56	66	546.	0.001
17	18	565.	0.130	57	67	546.	0.001
18	19	548.	0.034	58	68	546.	0.001
19	20	545.	0.002	59	69	545.	0.001
20	21	546.	0.004	60	70	583.	0.130
21	23	563.	0.109	61	72	595.	0.187
22	24	547.	0.031	62	73	574.	0.150
23	26	546.	0.002	63	74	569.	0.114
24	28	563.	0.097	64	75	559.	0.053
25	32	563.	0.114	65	76	596.	0.202
26	33	571.	0.156	66	77	578.	0.192
27	34	546.	0.012	67	78	585.	0.197
28	35	546.	0.002	68	79	545.	0.002
29	36	546.	0.004	69	80	545.	0.001
30	37	565.	0.081	70	81	545.	0.004
31	38	572.	0.133	71	82	607.	0.149
32	41	569.	0.072	72	84	589.	0.171
33	42	566.	0.101	73	85	585.	0.171
34	43	-	-	74	86	571.	0.123
35	44	547.	0.002	75	87	559.	0.061
36	45	547.	0.001	76	88	565.	0.050
37	46	565.	0.068	77	89	545.	0.002
38	47	562.	0.115	78	90	545.	0.007
39	48	577.	0.055	79	91	561.	0.057
40	49	567.	0.081	80	92	558.	0.050

REFERENCES

1. Tischler, A. O.: Defining a Giant Step in Space Transportation. Astronautics and Aeronautics, vol. 9, no. 2, Feb. 1971, pp. 22-25.

2. Marvin, J.G.; Lockman, W.K.; Mateer, G.G.; Seegmiller, H.L.; Pappas, C.C.: DeRose, C.E.; and Kaattari, G.E.: Flow Fields and Aerodynamic Heating of Space Shuttle Orbiters. NASA Space Shuttle Technology Conference. NASA TMX-52876, vol. 1, April 1971, pp. 21-73.

3. Marvin, J.G.; Seegmiller, H.L.; Lockman, W.K.; Mateer, G.G.; Pappas, C.C.; and DeRose, C.E.: Surface Flow Patterns and Aerodynamic Heating on Space Shuttle Vehicles. Paper No. 71-594, AIAA, June, 1971.

4. Seegmiller, H. Lee: Surface-Flow Visualization of a Delta Wing Shuttle Configuration at a Mach Number of 7.4 and Several Reynolds Numbers. NASA TM X-62,036, 1971.

5. Holdaway, George H.; Polek, Thomas E.; and Kemp, Joseph H., Jr.: Aerodynamic Characteristics of a Blunt Half-Cone Entry Configuration at Mach Numbers of 5.2, 7.4, and 10.4. NASA TM X-682, 1963.

6. Fay, J.A.; and Riddell, F.R.: Theory of Stagnation Point Heat Transfer in Dissociated Air. J. Aeron. Sci., vol. 25, no. 1, Feb. 1958, pp. 73-85.

7. Bertram, Mitchel H.: Comment on "Viscosity of Air". J. Spacecraft Rockets, vol. 4, no. 2, Feb. 1967, pp. 287-288.

8. Ames Research Staff: Equations, Tables, and Charts for Compressible Flow. NACA Rep. 1135, 1953.

9. Beckwith, Ivan E.; and Cohen, Nathaniel B.: Application of Similar Solutions to Calculation of Laminar Heat Transfer on Bodies with Yaw and Large Pressure Gradient in High-Speed Flow. NASA TN D-625, 1961.

10. Beckwith, Ivan E.; and Gallagher, James J.: Local Heat Transfer and Recovery Temperatures on a Yawed Cylinder at a Mach Number of 4.15 and High Reynolds Numbers. NASA TR R-104, 1961.

11. Inouye, Mamoru; Marvin, Joseph G.; and Sinclair, A.R.: Comparison of Experimental and Theoretical Shock Shapes and Pressure Distributions on Flat-Faced Cylinders at Mach 10.5. NASA TN D-4397, 1968.

12. Bertram, Mitchel H.; and Henderson, Arthur, Jr.: Recent Hypersonic Studies of Wings and Bodies. ARS J., vol 31, no. 8, Aug. 1961, pp. 1129-1139.

13. Korkegi, Robert H.: Survey of Viscous Interactions Associated with High Mach Number Flight, AIAA J., vol 9, no. 5, May 1971, pp. 771-784.

TABLE I

THERMOCOUPLE LOCATIONS

DELTA-WING ORBITER

(a) BODY

T/C No.	X/L	∅, deg	T/C No.	X/L	∅, deg
1	0	0	26	.40	180
2	.01	↓	27	.45	0
3	.02	↓	28	.50	↓
4	.03	↓	29	↓	105
5	↓	180	30	↓	180
6	.04	0	31	.55	0
7	.10	↓	32	.60	↓
8	↓	106	33	↓	79
9	↓	180	34	↓	103
10	.20	0	35	↓	142
11	↓	104	36	↓	180
12	↓	180	37	.70	0
13	.22	↓	38	↓	79
14	.24	↓	39	↓	103
15	.26	0	40	↓	180
16	↓	158	41	.80	0
17	↓	180	42	↓	76
18	.30	0	43	↓	102
19	↓	106	44	↓	139
20	↓	158	45	↓	180
21	↓	180	46	.90	0
22	.35	0	47	↓	79
23	.40	↓	48	.992	0
24	↓	105	49	↓	78
25	↓	144	50	↓	180

TABLE I. - Concluded

THERMOCOUPLE LOCATIONS

DELTA-WING ORBITER

(b) WING

T/C No.	% Exposed Semispan	% Chord	Wing Designation
51	7.0	10	right, top
52	↓	20	↓
53		40	
54		60	
55	↓	80	↓
56	16.7	20	
57	↓	40	
58		60	
59		80	↓
60		2.5	left, bottom
61		5	↓
62		20	
63		40	
64		60	
65	↓	80	↓
66	45.6	10	right, top
67	↓	20	↓
68		40	
69		80	↓
70		2.5	left, bottom
71		5	↓
72		10	
73		20	
74		40	
75	↓	80	↓
76	55.3	10	
77	65.0	↓	
78	74.6		↓
79	84.3	20	right, top
80	↓	40	↓
81		80	
82		2.5	left, bottom
83		5	↓
84		10	
85		20	
86		40	
87	↓	80	↓

(c) TWIN VERTICAL TAILS

T/C No.	% Exposed Height	% Chord	Tail Designation
88	20	10	left, outboard
89	↓	40	right, inboard
90	50	↓	↓
91	70	10	left, outboard
92	↓	40	↓

TABLE II

THERMOCOUPLE CONNECTION SCHEDULE

DELTA-WING ORBITER

(Test 106 : Runs 1 - 16, 18 - 26, 54 - 60, and 66)

Channel No.	T/C No.	Location
1	1	body
2	2	
3	3	
4	4	
5	5	
6	6	
7	7	
8	8	
9	9	
10	10	
11	11	
12	12	
13	13	
14	14	
15	16	
16	17	
17	18	
18	19	
19	20	
20	21	
21	23	
22	24	
23	26	
24	28	
25	32	
26	33	
27	34	
28	35	
29	36	
30	37	
31	38	
32	41	
33	42	
34	43	
35	44	
36	45	
37	46	
38	47	
39	48	
40	49	

Channel No.	T/C No.	Location
41	50	body
42	51	wing
43	52	
44	53	
45	54	
46	55	
47	56	
48	57	
49	58	
50	59	
51	60	
52	62	
53	63	
54	64	
55	65	
56	66	
57	67	
58	68	
59	69	
60	70	
61	72	
62	73	
63	74	
64	75	
65	76	
66	77	
67	78	
68	79	
69	80	
70	81	
71	82	
72	84	
73	85	
74	86	
75	87	
76	88	tail
77	89	
78	90	
79	91	
80	92	

TABLE III

RUN SCHEDULE

DELTA-WING ORBITER

(Test 106: Runs 1 - 16, 18 - 26, 54 - 60, and 66)

$M_\infty = 7.4$

Run	α, deg	β, deg	δ_e, deg	δ_r, deg	$Re_{\infty,L}$
55	-5	0	0	0	$.75 \times 10^6$
57	↓	↓	↓	↓	3.71
54	0				.67
56	↓				3.57
1	15				1.14
2					3.88
18					6.21
60			↓	↓	7.34
19			+14	±20	.85
20		↓	↓	↓	3.98
21		-5			1.09
22	↓	↓	↓	↓	4.35
59	20	0	0	0	7.23
66	25				7.00
3	30				1.04
4					2.12
5					3.06
6					4.17
58			↓	↓	7.24
14			+10	±13	1.00
15					2.52
16		↓	↓	↓	4.20
23		-5			1.06
24	↓	↓	↓	↓	4.37
7	53	0	0	0	1.21
8					1.83
9					3.17
10			↓		4.29
11			-7.5		1.10
12					2.49
13		↓	↓	↓	3.98
25		-5			1.10
26	↓	↓	↓	↓	4.22

L = 0.323 meter (12.720 in.)
0.006 Model Scale

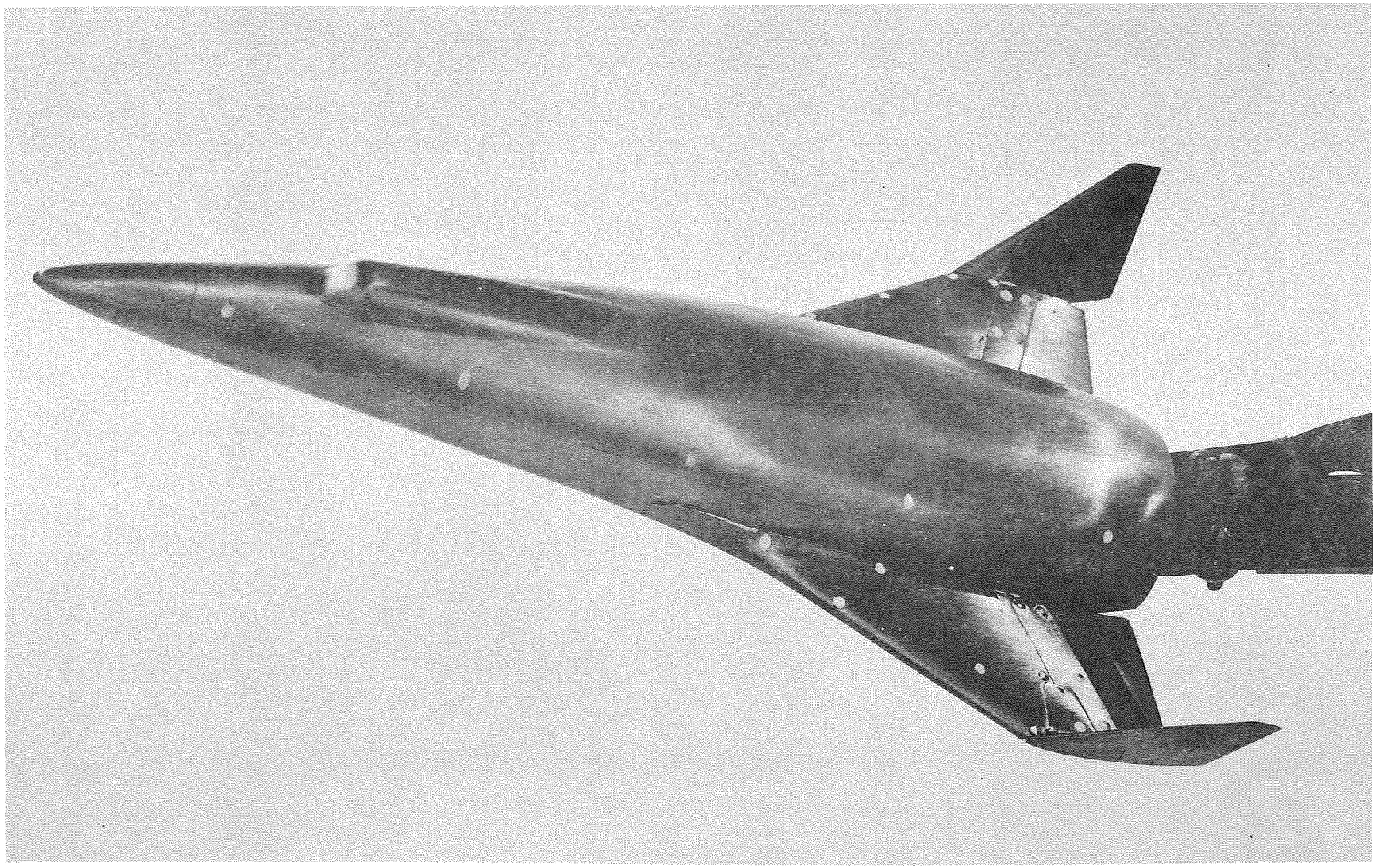

Figure 1. - Photograph of delta-wing orbiter model mounted on support bracket.

NATIONAL AERONAUTICS AND SPACE ADMINISTRATION
AMES RESEARCH CENTER, MOFFETT FIELD, CALIFORNIA

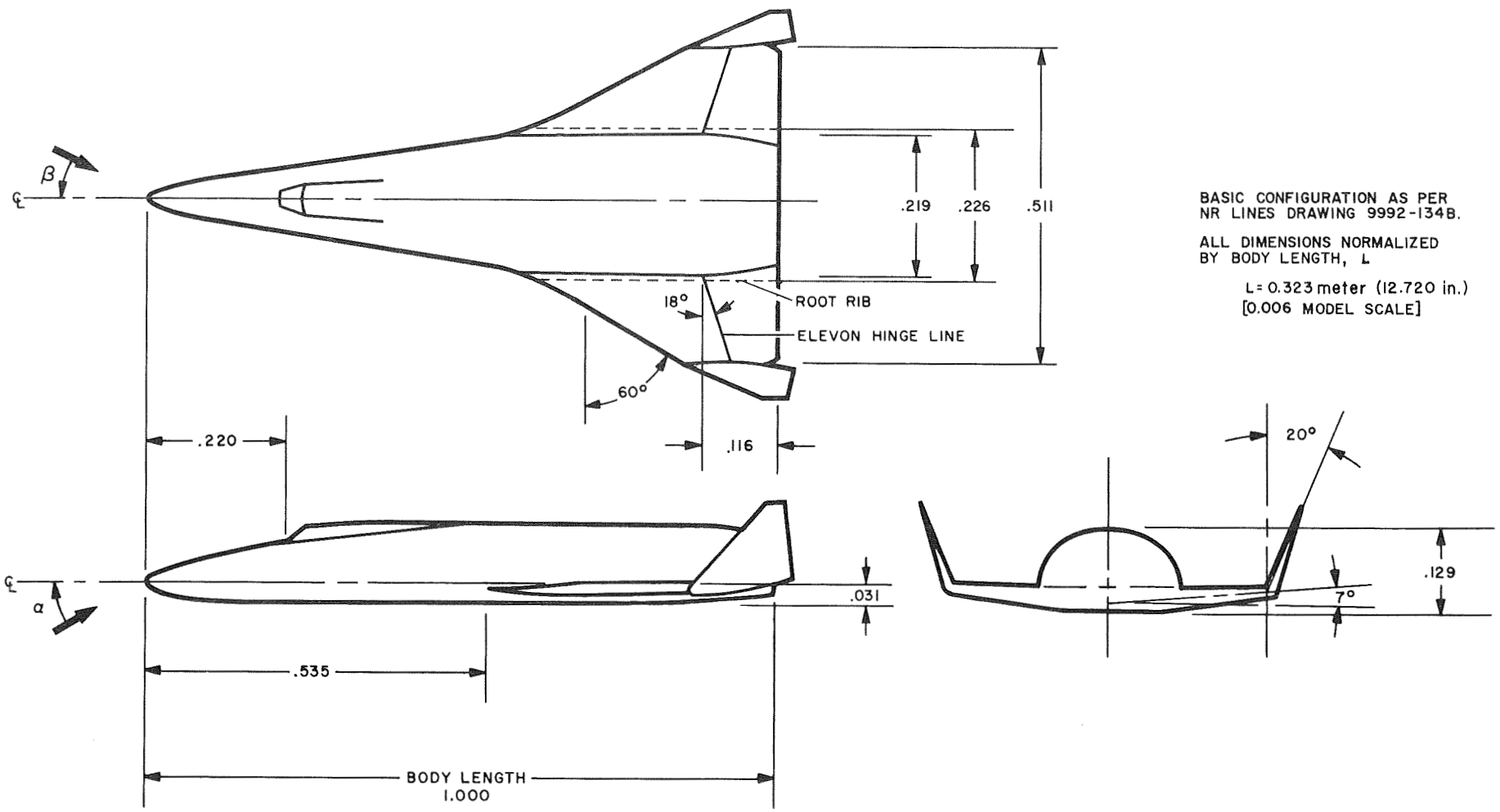

Figure 2. - Three-view drawing of delta-wing orbiter model with flow orientation.

NATIONAL AERONAUTICS AND SPACE ADMINISTRATION
AMES RESEARCH CENTER, MOFFETT FIELD, CALIFORNIA

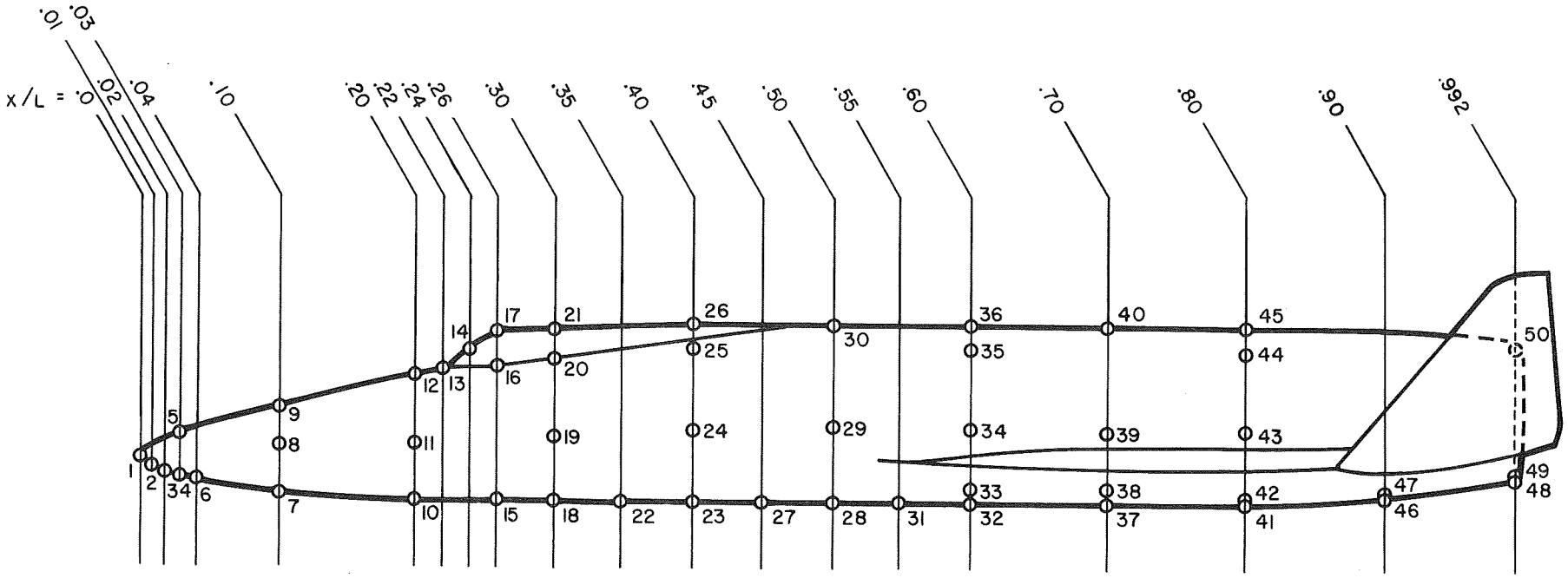

(a) Body.

Figure 3. - Thermocouple locations for delta-wing orbiter model.

NATIONAL AERONAUTICS AND SPACE ADMINISTRATION
AMES RESEARCH CENTER, MOFFETT FIELD, CALIFORNIA

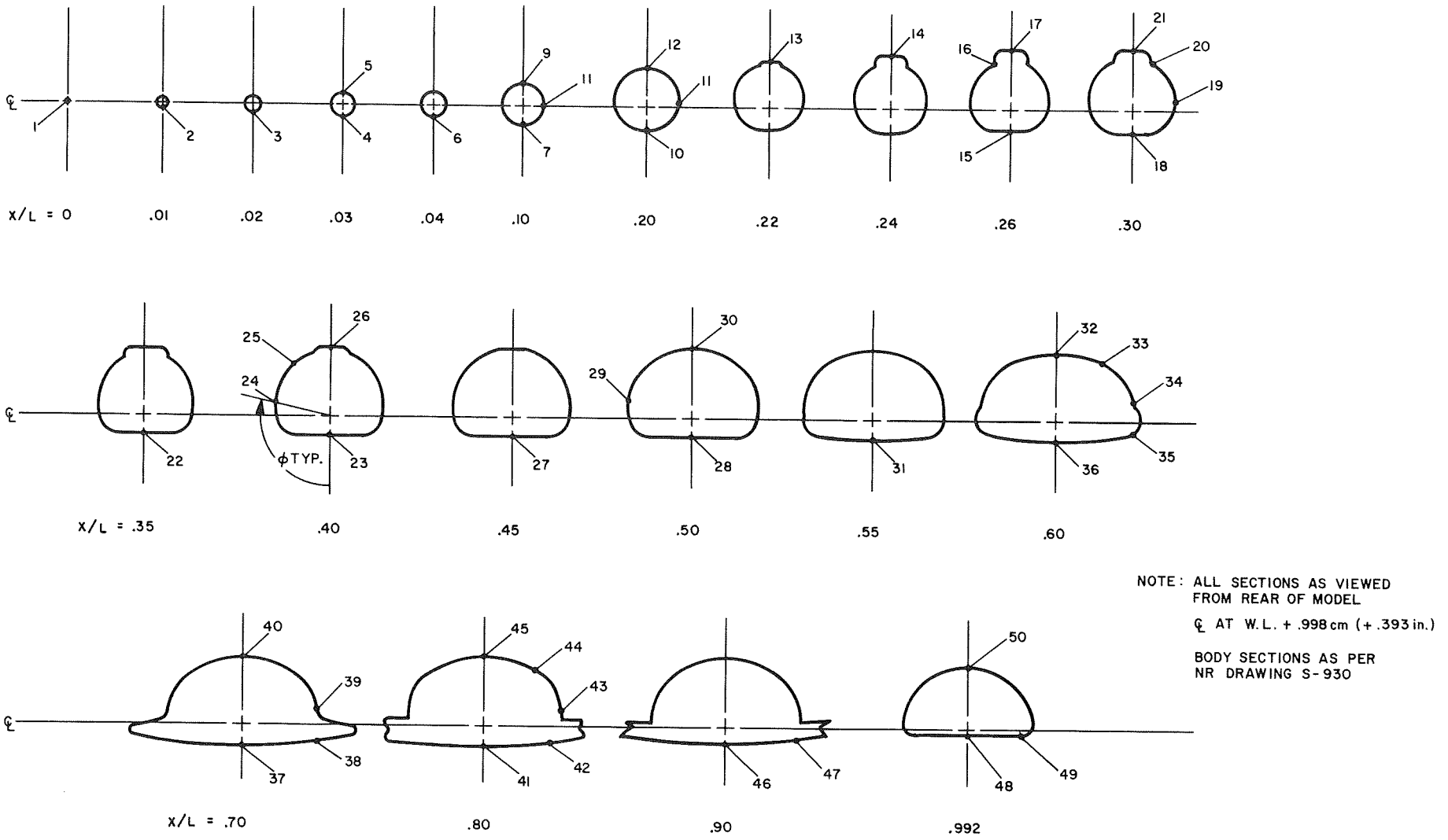

(b) Body cross sections.

Figure 3. - Continued.

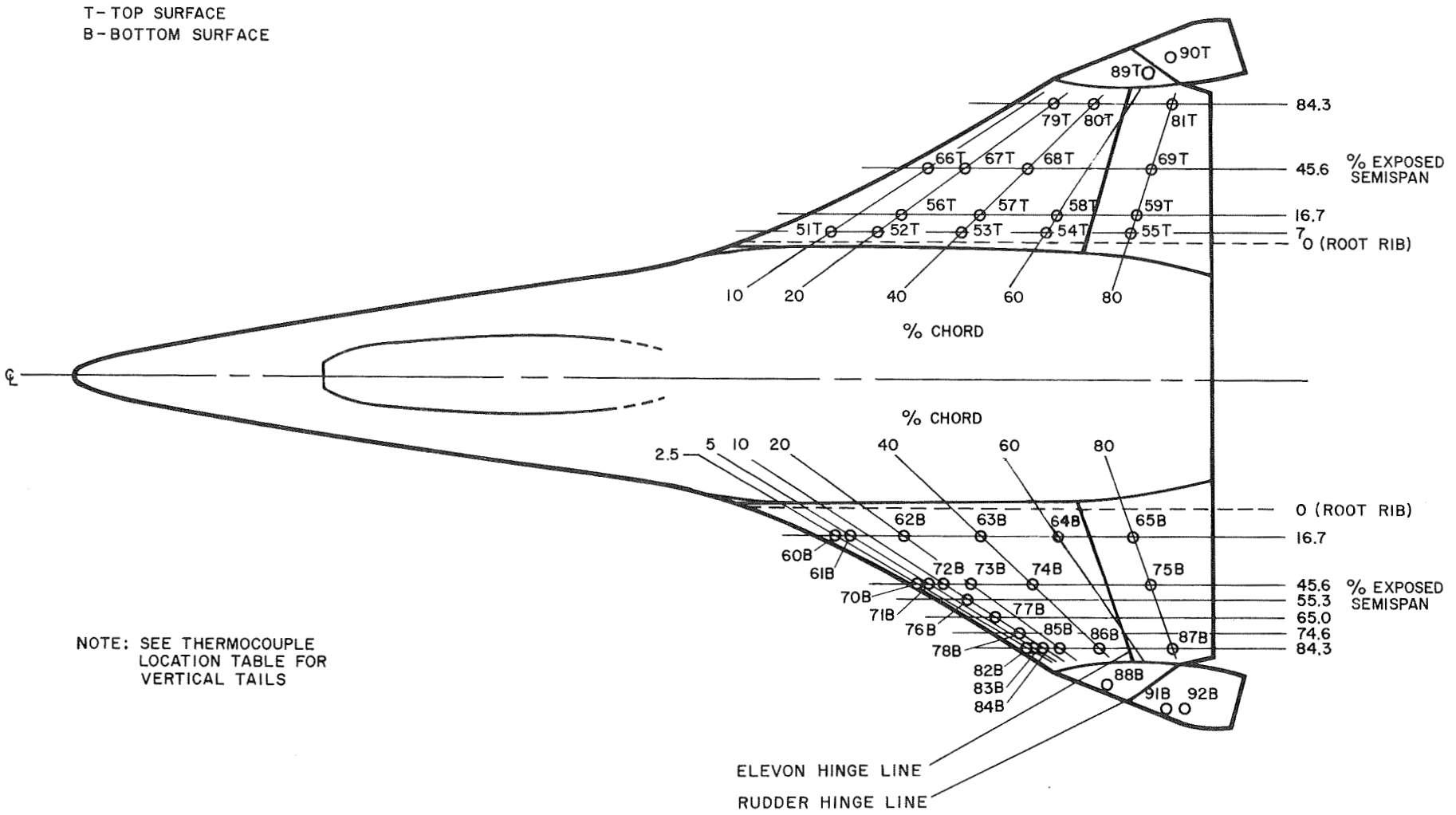

(c) Wing and twin vertical tails.

Figure 3. - Concluded.

NATIONAL AERONAUTICS AND SPACE ADMINISTRATION
AMES RESEARCH CENTER, MOFFETT FIELD, CALIFORNIA

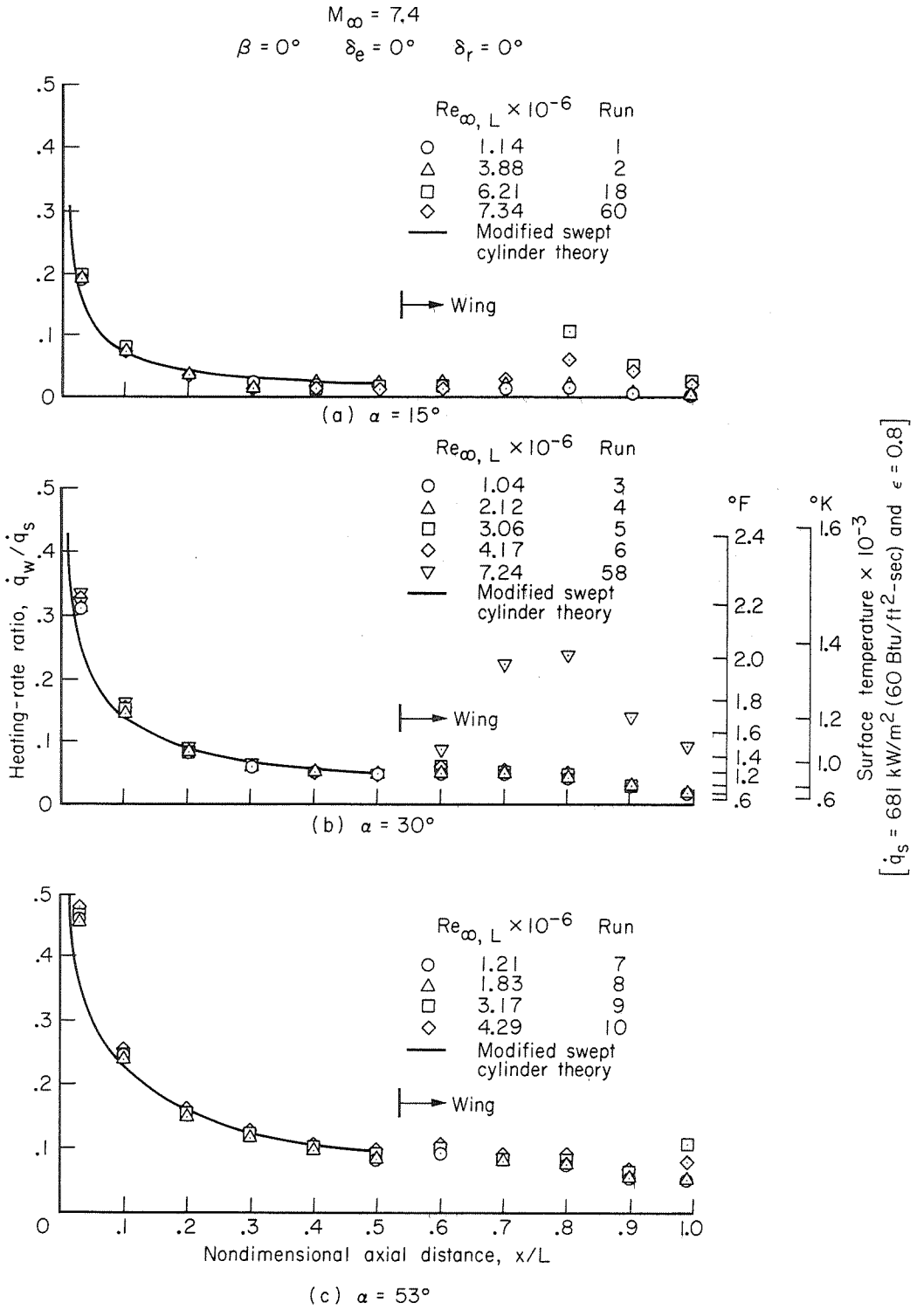

Figure 4. - Body bottom-centerline heating.

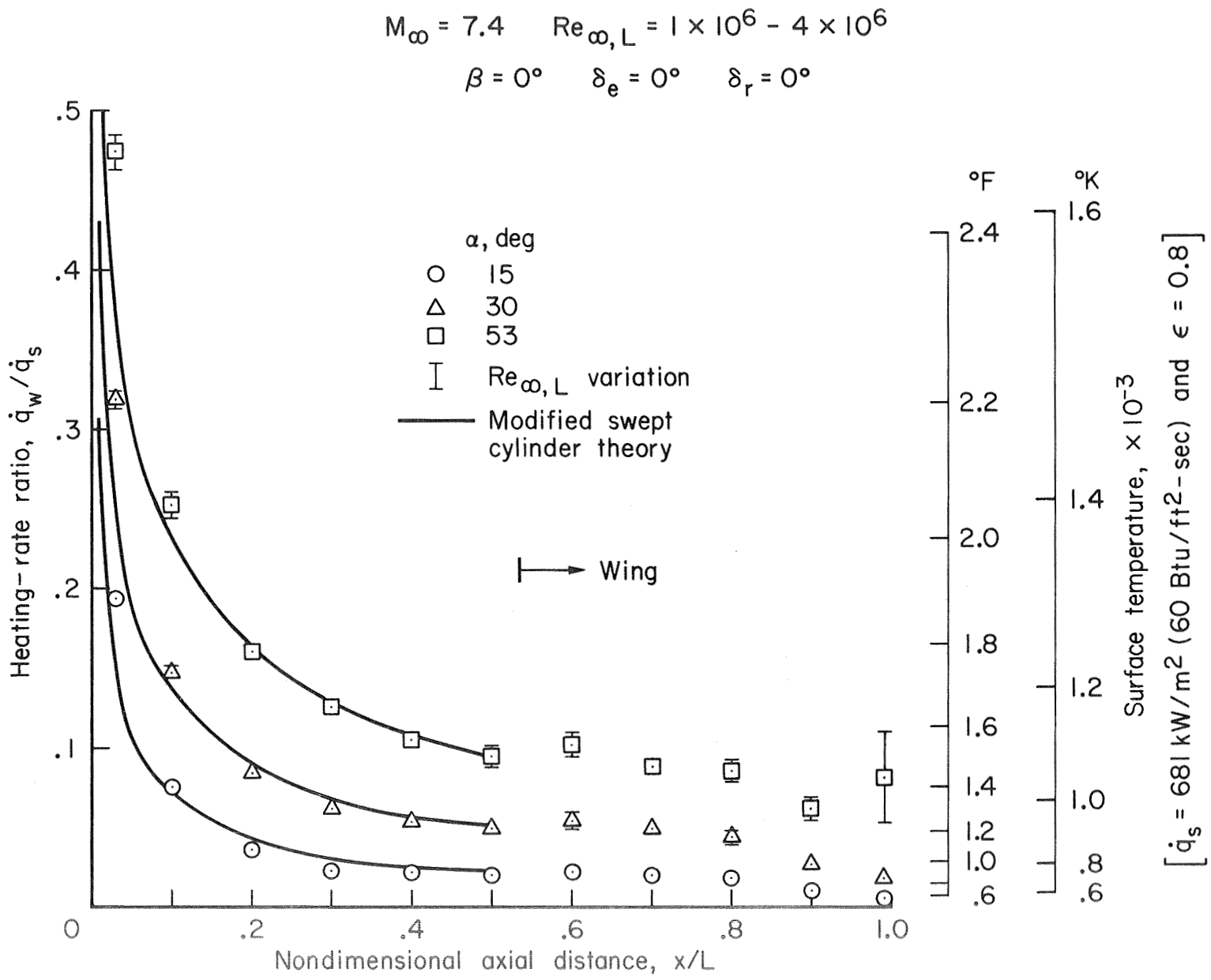

Figure 5. - Effect of angle of attack on body bottom-centerline heating for $Re_{\infty,L} = 1 \times 10^6 - 4 \times 10^6$.

NATIONAL AERONAUTICS AND SPACE ADMINISTRATION
AMES RESEARCH CENTER, MOFFETT FIELD, CALIFORNIA

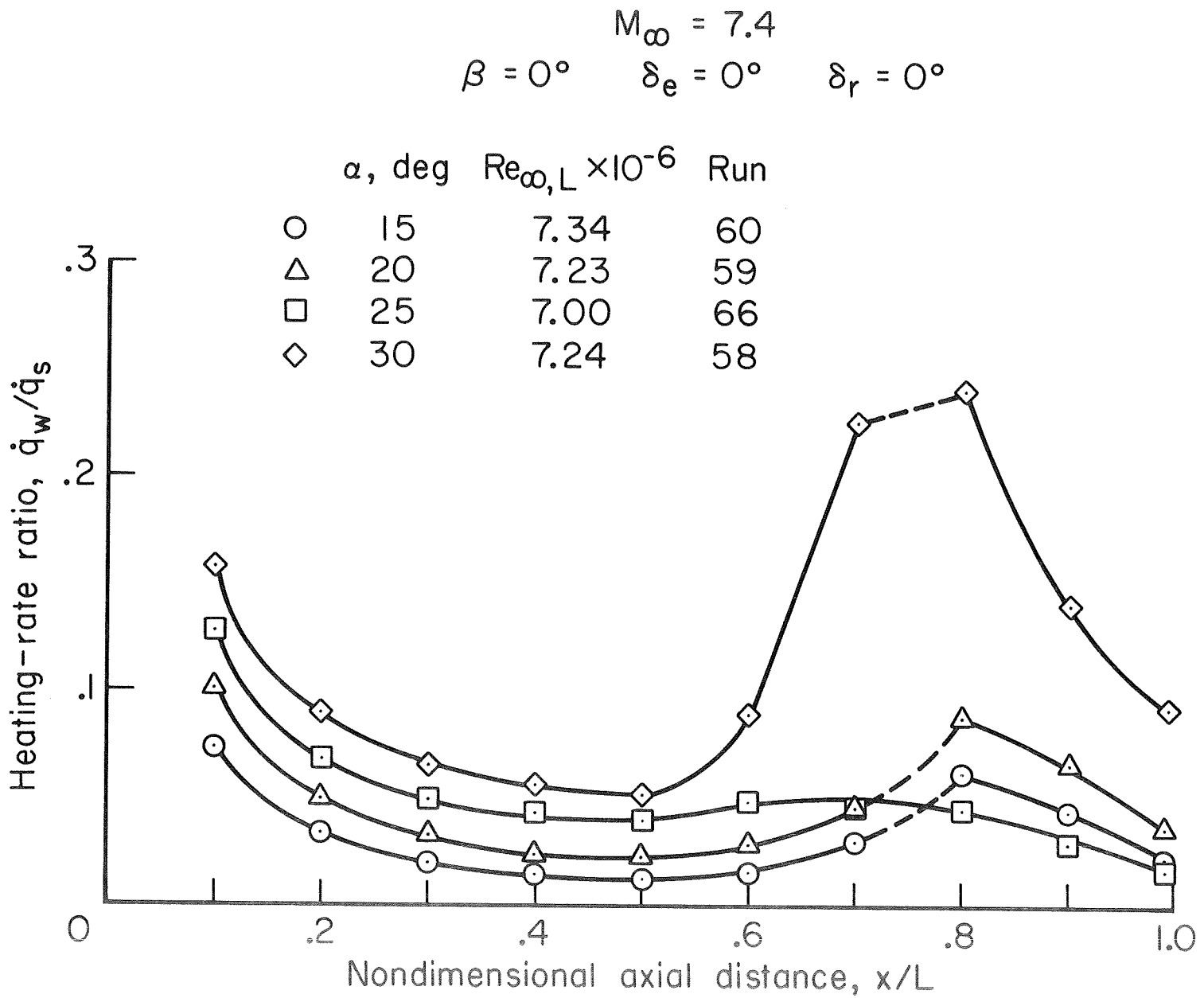

Figure 6. - Effect of angle of attack on body bottom-centerline heating for $Re_{\infty,L} = 7 \times 10^6$.

NATIONAL AERONAUTICS AND SPACE ADMINISTRATION
AMES RESEARCH CENTER, MOFFETT FIELD, CALIFORNIA

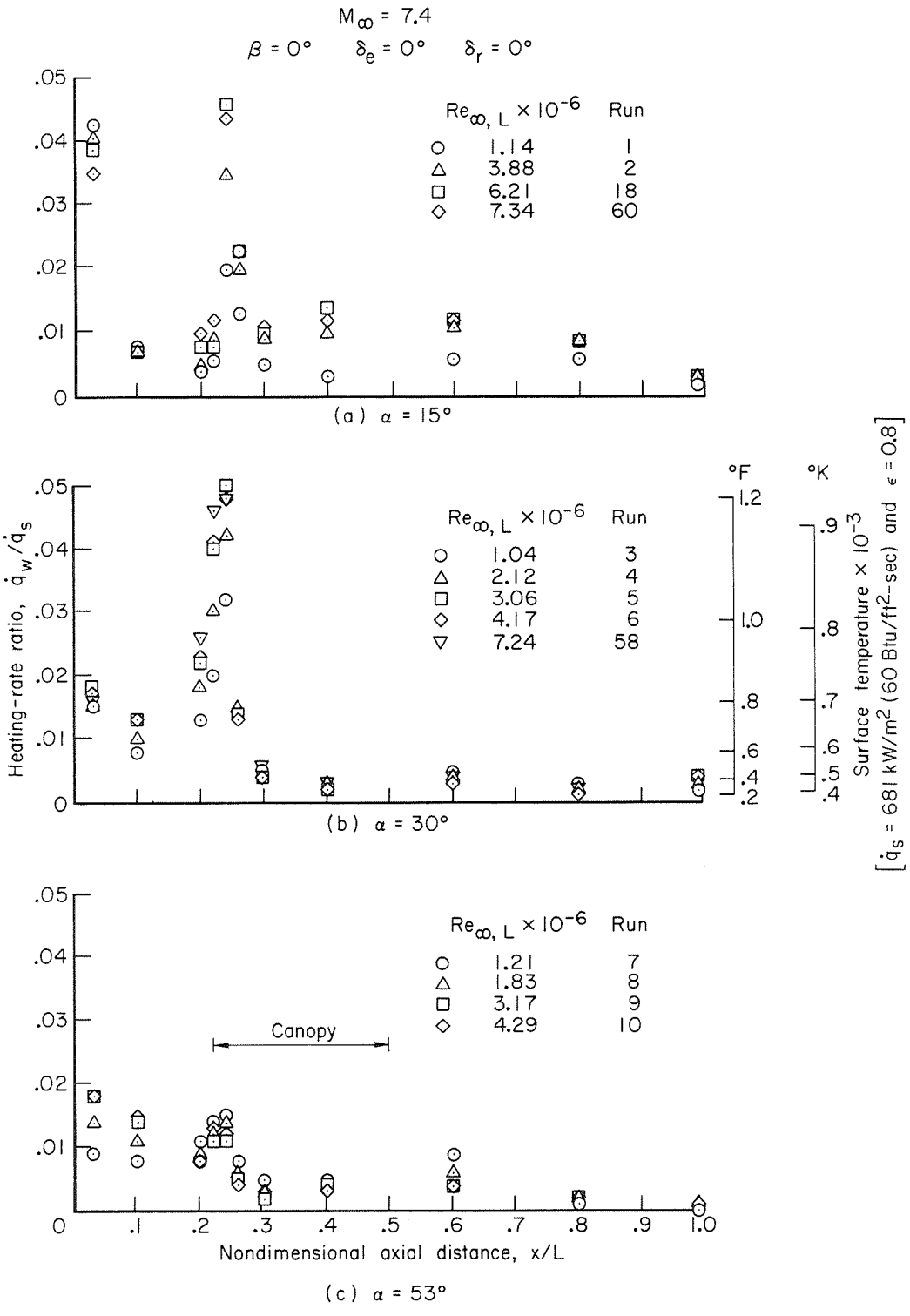

Figure 7. - Body top-centerline heating.

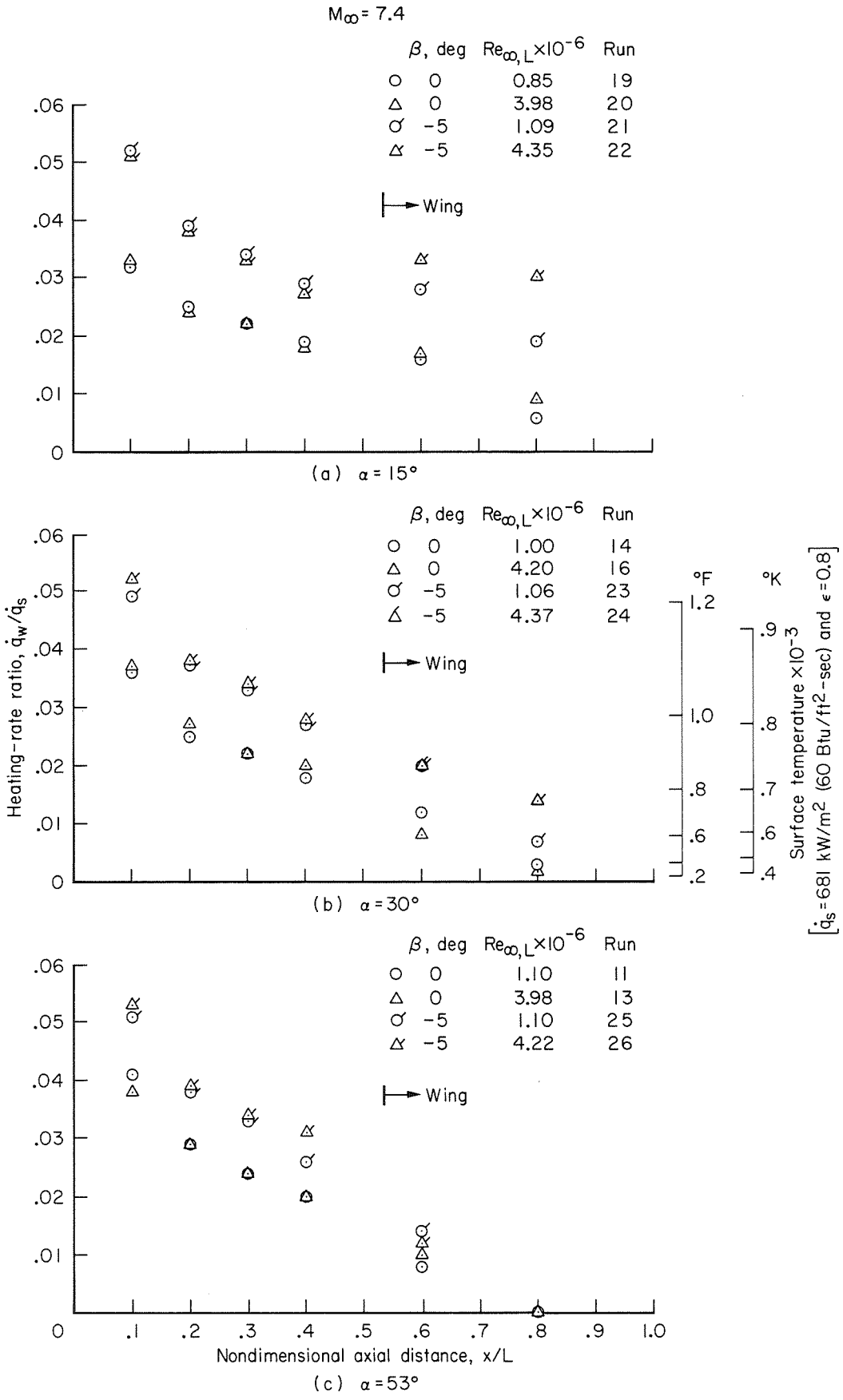

Figure 8. - Effect of sideslip on body side ($\phi \gtrsim 100^\circ$) heating.

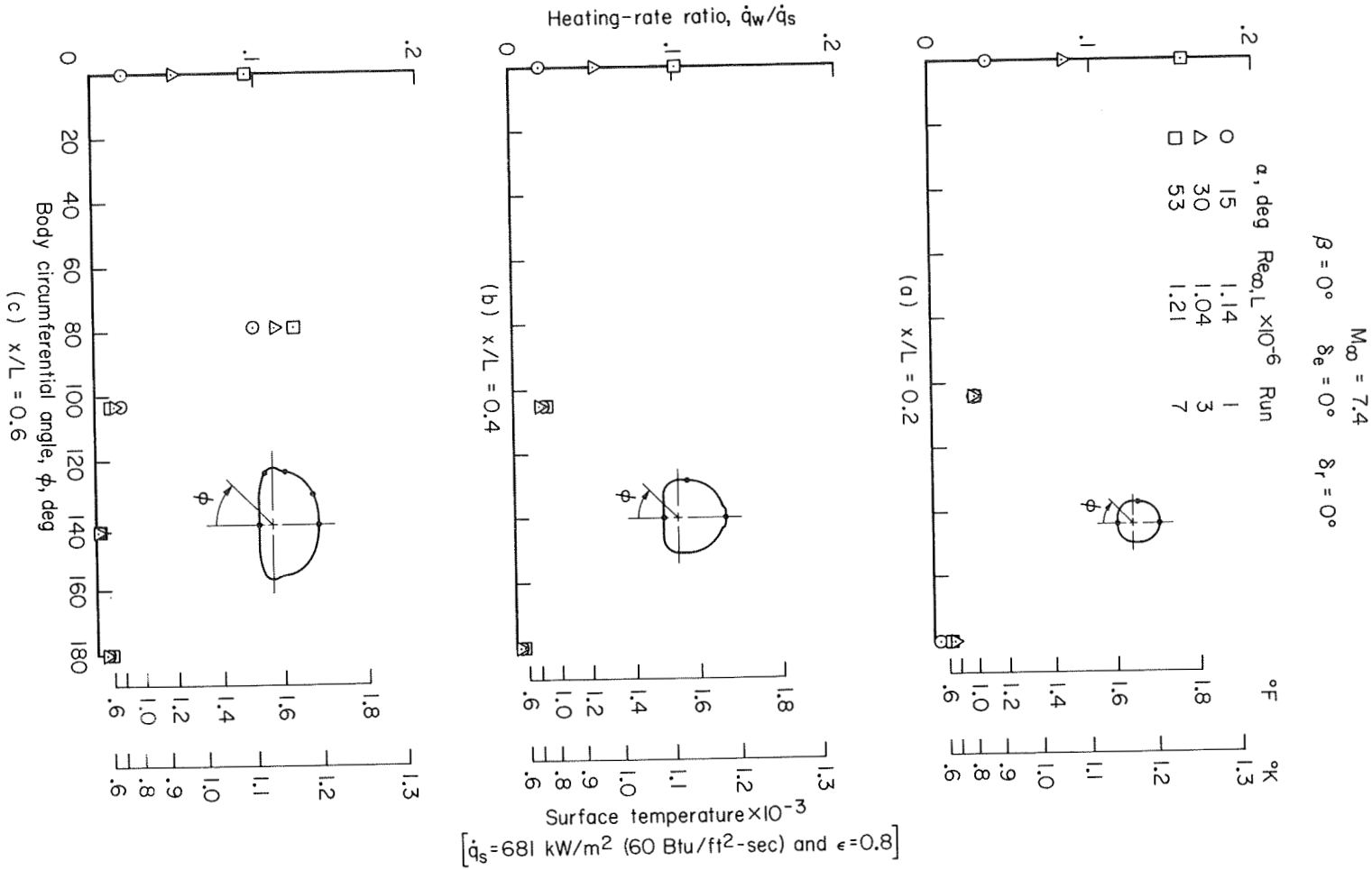

Figure 9. - Body cross-section heating.

NATIONAL AERONAUTICS AND SPACE ADMINISTRATION
AMES RESEARCH CENTER, MOFFETT FIELD, CALIFORNIA

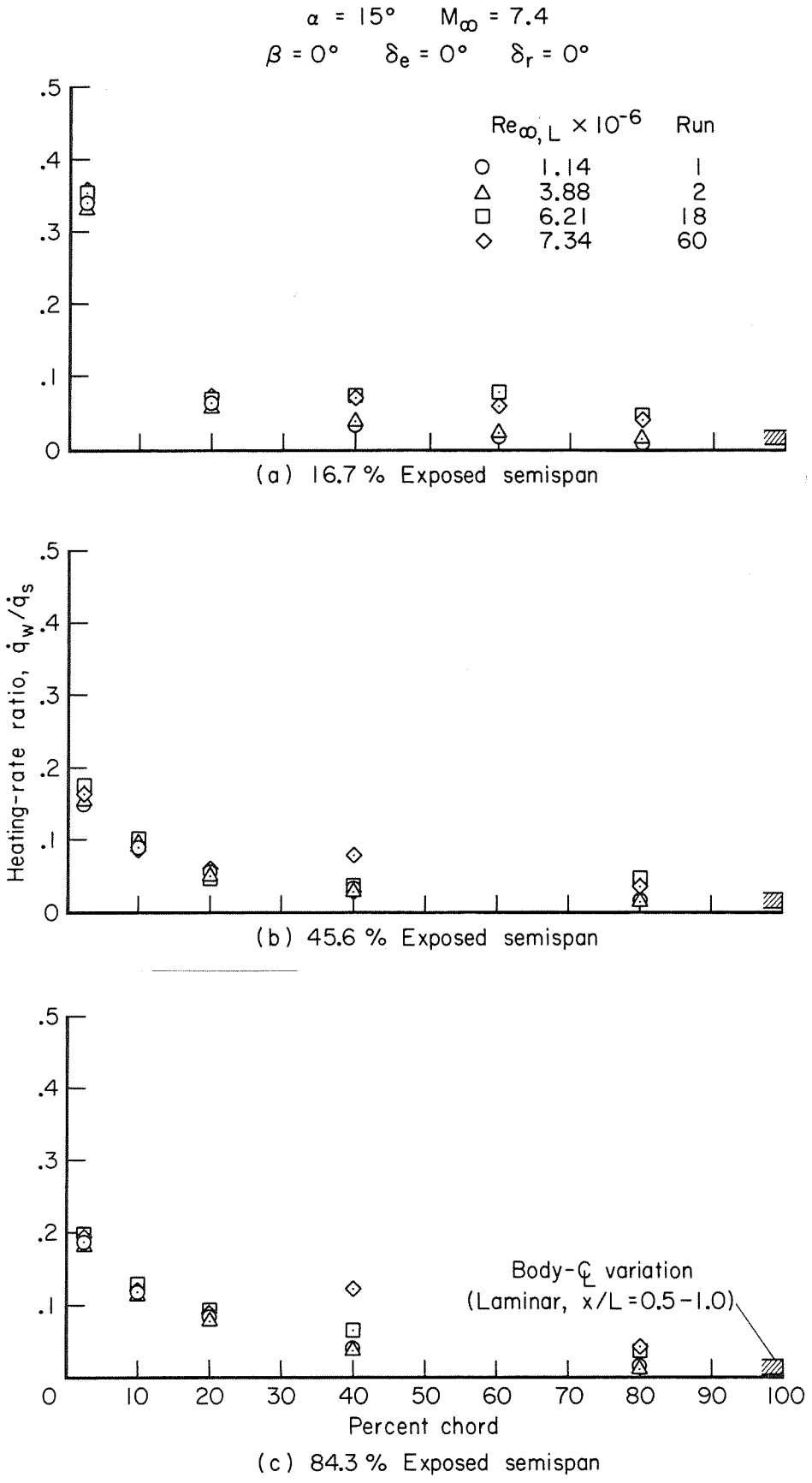

Figure 10. - Wing bottom-surface chordwise heating at $\alpha = 15^{\circ}$.

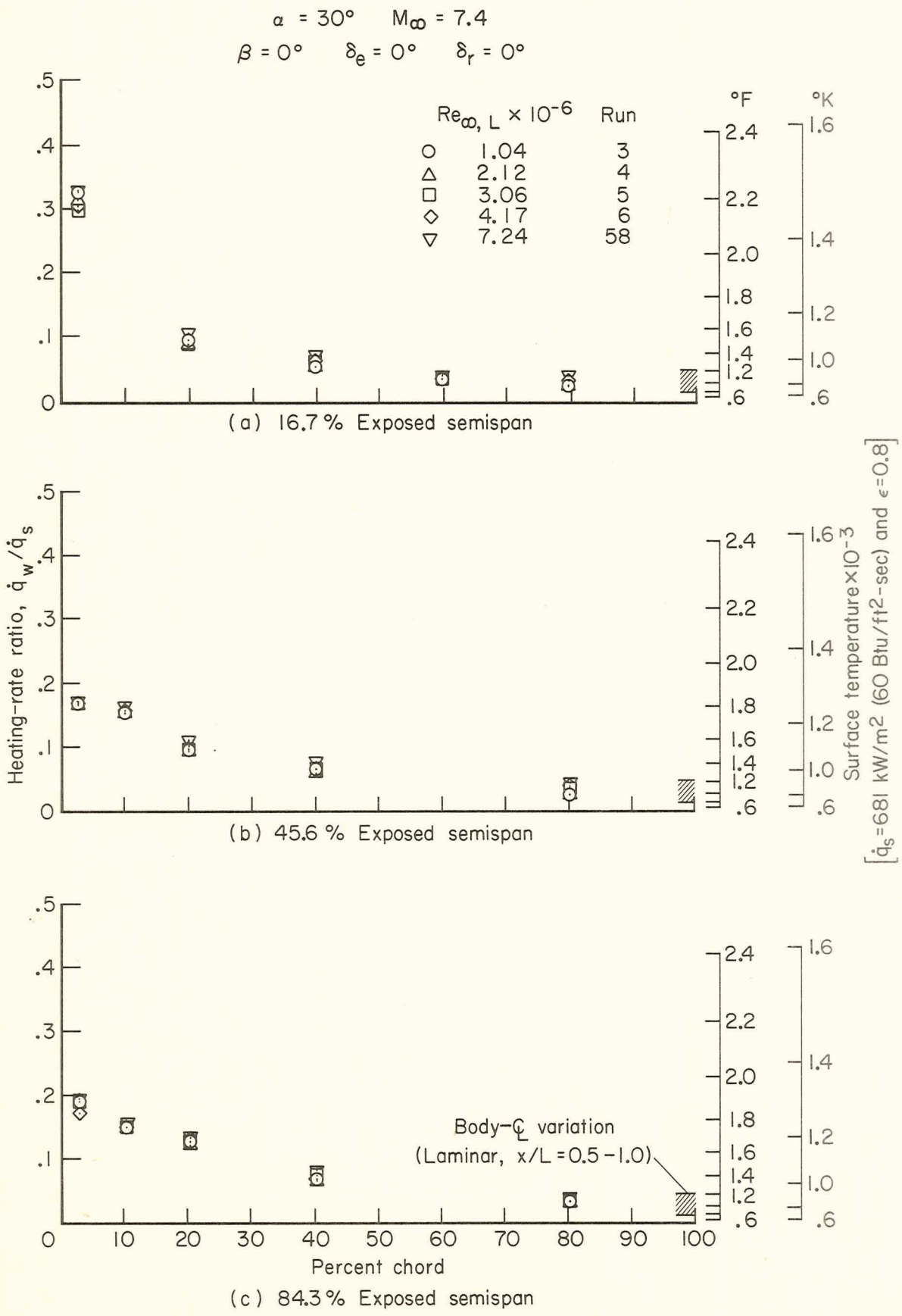

Figure 11. - Wing bottom-surface chordwise heating at $\alpha = 30^{\circ}$.

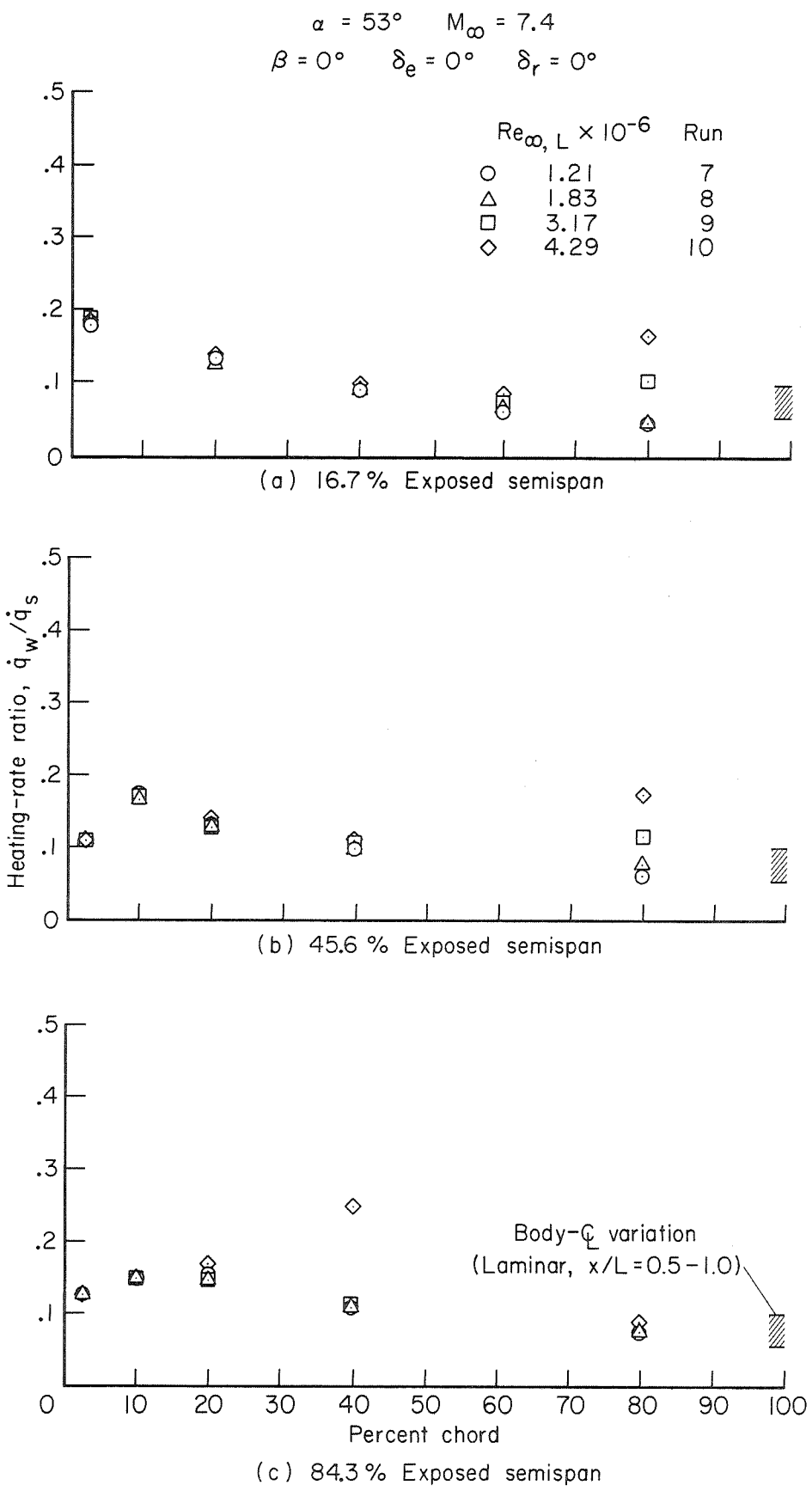

Figure 12. - Wing bottom-surface chordwise heating at $\alpha = 53^{\circ}$.

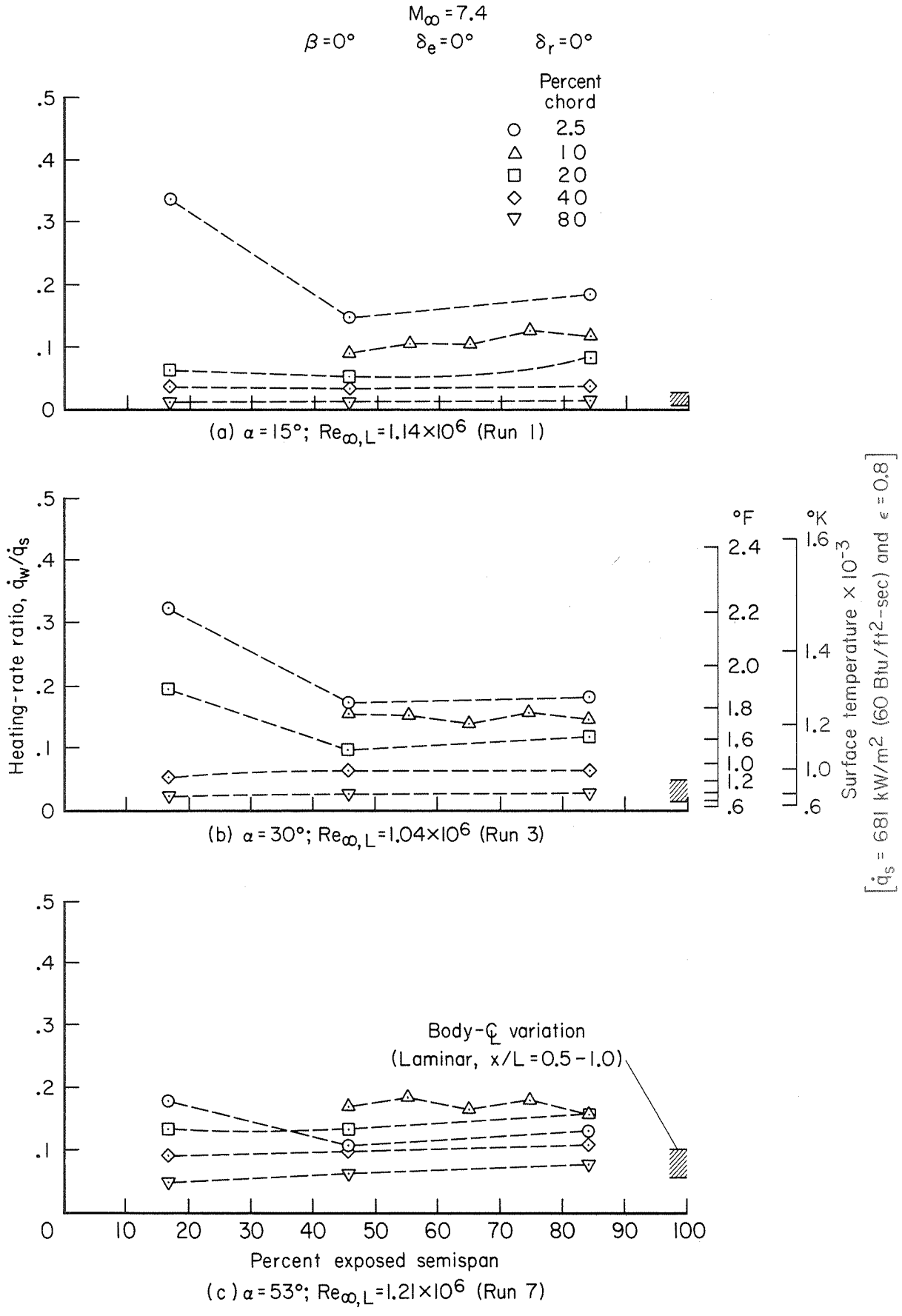

Figure 13. - Wing bottom-surface spanwise heating for $Re_{\infty,L} = 1 \times 10^6$.

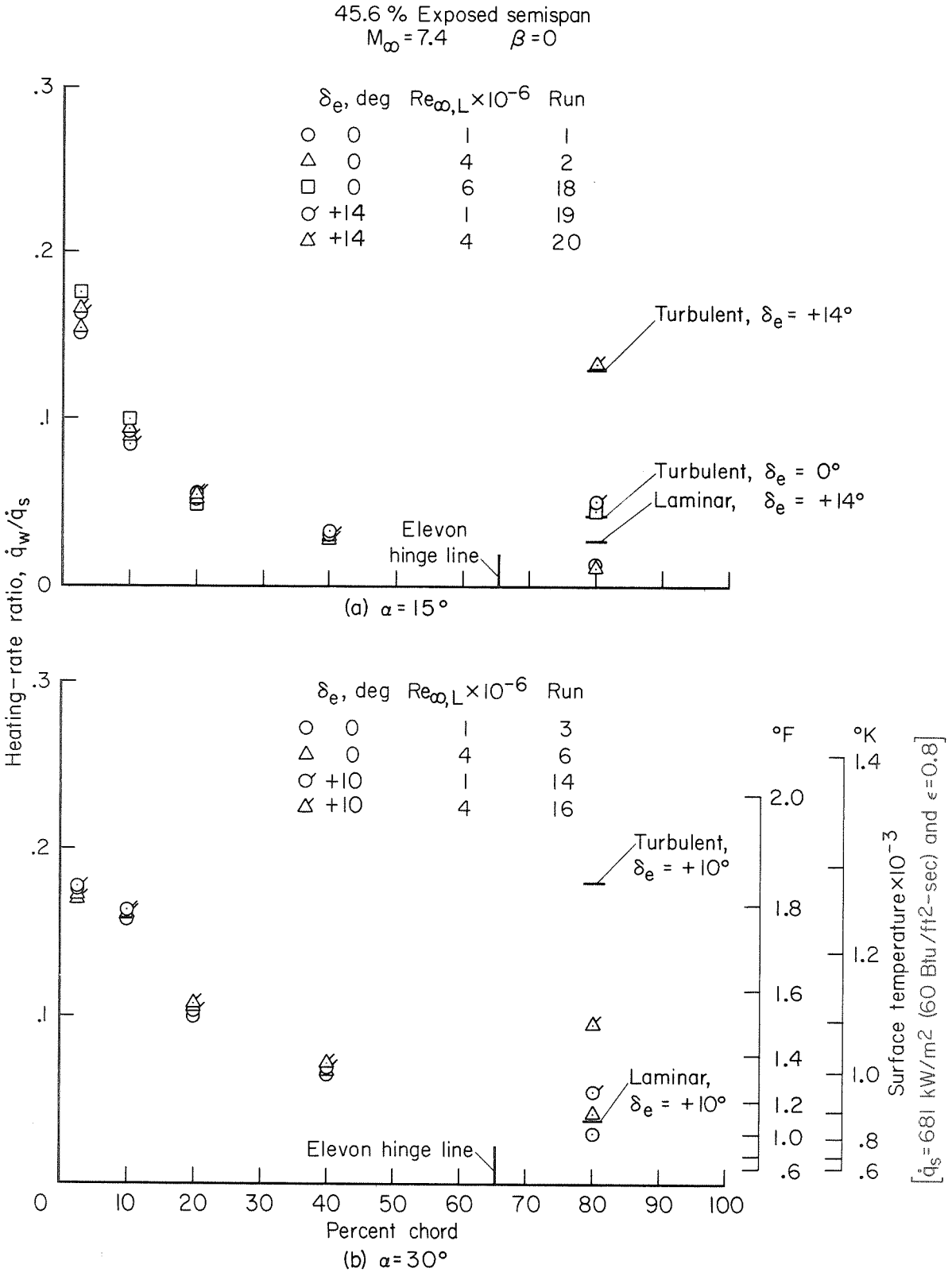

Figure 14. - Effect of elevon deflection on wing bottom-surface heating.

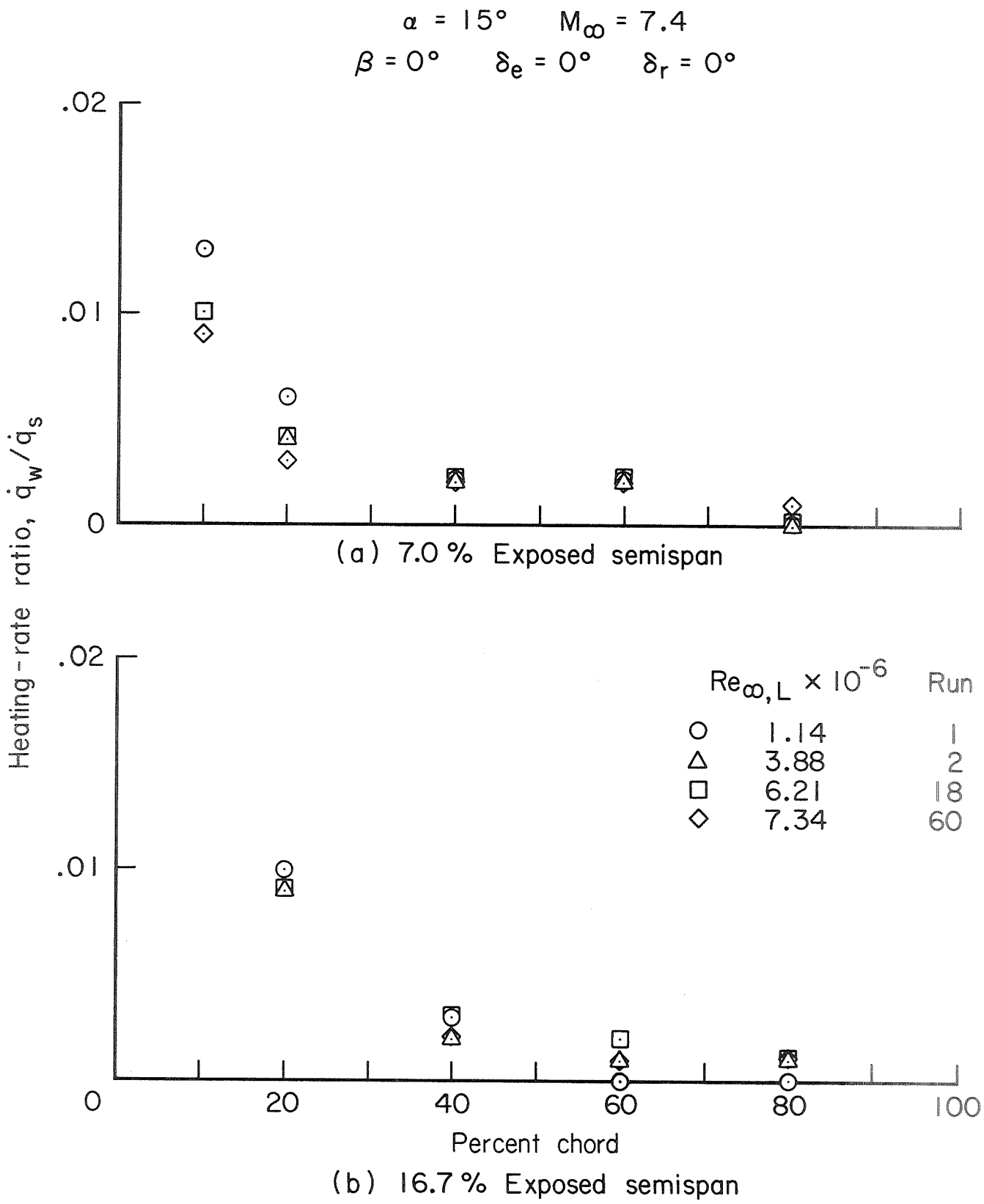

Figure 15. - Wing top-surface chordwise heating at α = 15°.

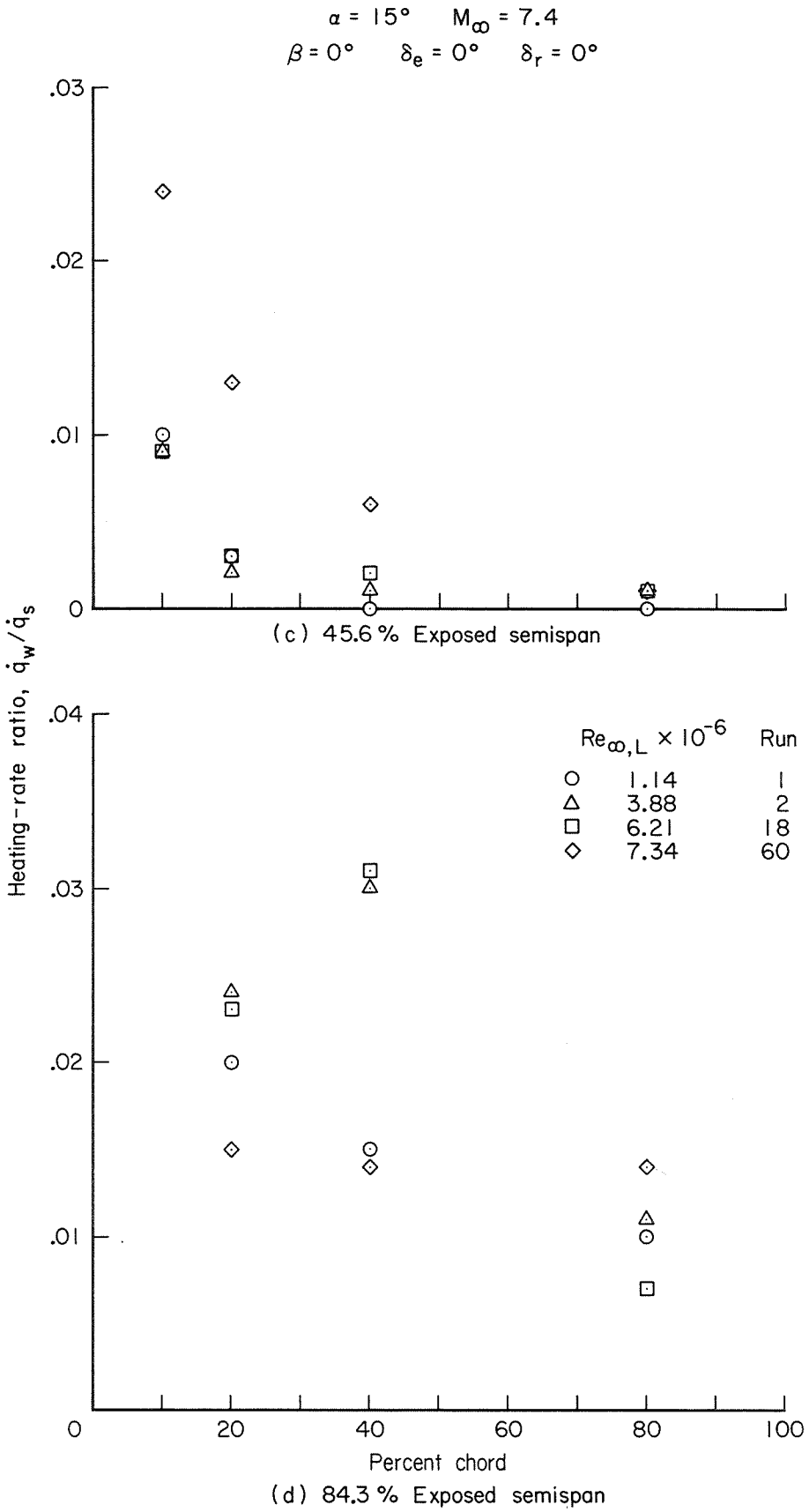

Figure 15. - Concluded.

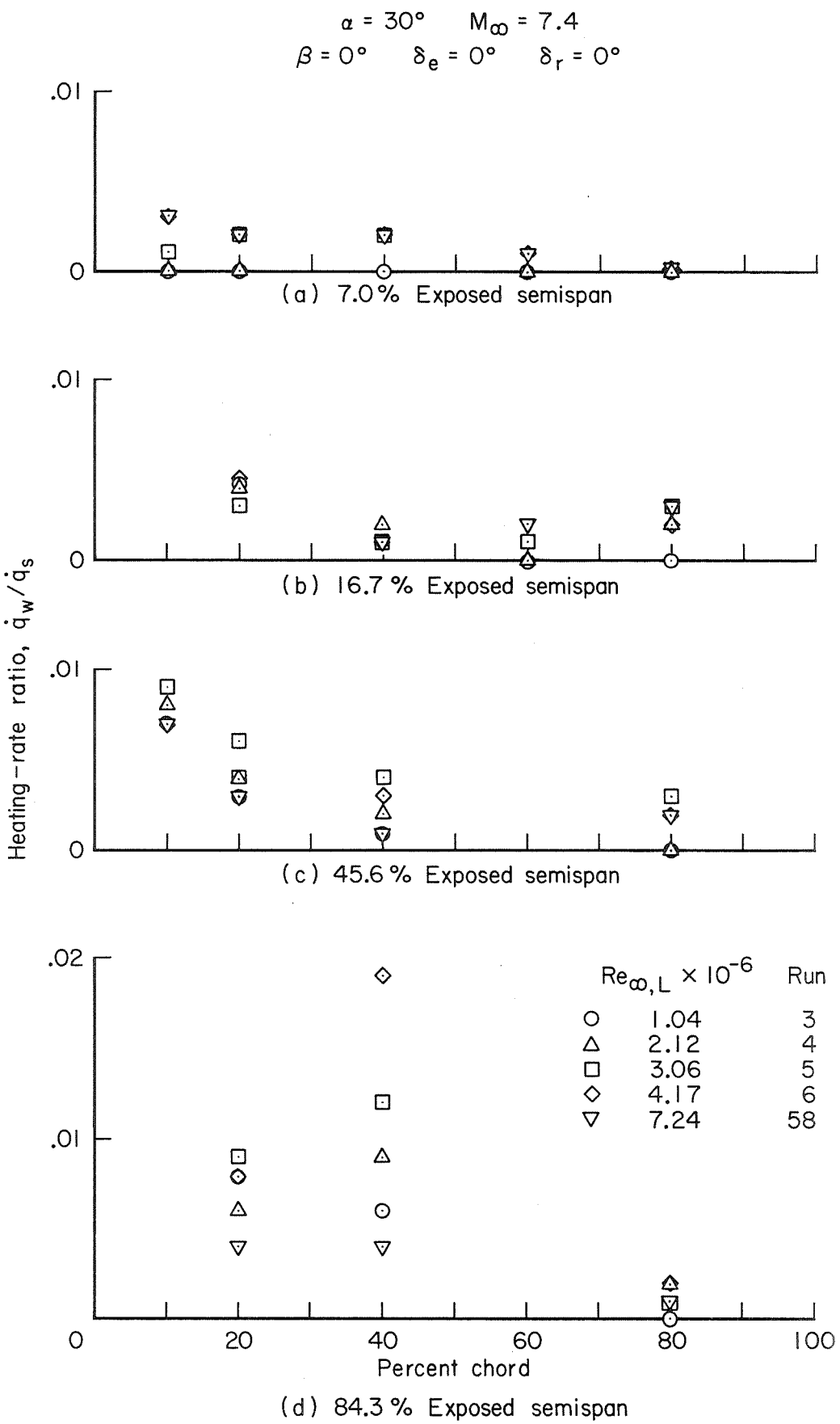

Figure 16. - Wing top-surface chordwise heating at $\alpha = 30^{\circ}$.

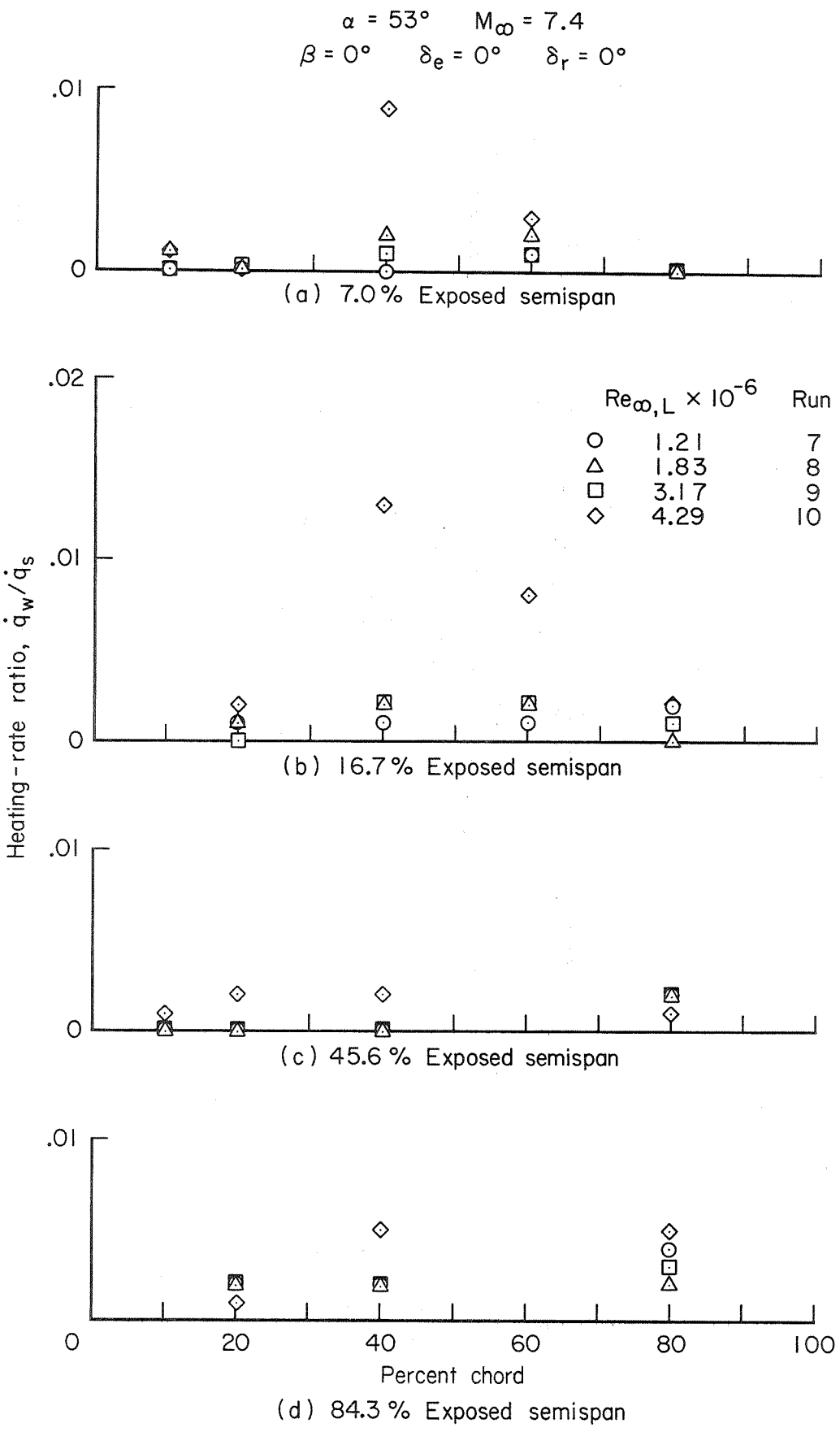

Figure 17. - Wing top-surface chordwise heating at $\alpha = 53^{\circ}$.